STUDY OF THE EFFECT OF SOME TYPES OF NUCLEAR RADIATION ON SOME PHYSICAL PROPERTIES OF A TIN OXIDE FILM

2024
MASTER THESIS
PHYSICS

Abdulrahman Faaiq Dawood AL-BADRY

Thesis Advisor
Assist. Prof. Dr. Khalid Hadi Mahdi AAL-SHABEEB

STUDY OF THE EFFECT OF SOME TYPES OF NUCLEAR RADIATION ON SOME PHYSICAL PROPERTIES OF TIN OXIDE FILM

Abdulrahman Faaiq Dawood AL-BADRY

Thesis Advisor
Assist. Prof. Dr. Khalid Hadi Mahdi AAL-SHABEEB

T.C.
Karabuk University
Institute of Graduate Program
Department of Physics
Prepared as
Master Thesis

KARABÜK
February 2024

Abdulrahman Faaiq Dawood AL-BADRY prepared by “STUDY OF THE EFFECT OF SOME TYPES OF NUCLEAR RADIATION ON SOME PHYSICAL PROPERTIES OF TIN OXIDE FILM” I certify that this thesis titled is suitable as a Master's Thesis.

Assist. Prof. Dr. Khalid Hadi Mahdi AAL-SHABEEB .....

Thesis supervisor, Physics Department

This thesis is accepted by the examining committee with a unanimous vote in the Department of Physics Department as a Master of Science thesis. 01/02/2024

Examining Committee Members (Institutions)	Signature
Chairman : Assist.Prof.Dr. Khalid AAL-SHABEEB (KBÜ.)	.....
Member : Prof. Dr. Aybaba HANÇERLİOĞULLARI (KÜ.)	.....
Member : Dr. Öğretim Üyesi Ulvi KANBUR (KBÜ.)	.....

The degree of Master of Science by the thesis submitted is approved by the Administrative Board of the Institute of Graduate Programs, Karabuk University.

Assoc. Prof. Dr. Zeynep ÖZCAN .....

Director of the Institute of Graduate Programs

"*All information in this letter has been obtained and provided by academic rules and ethical principles; I further certify that I have provided all attribution that does not arise in this work, as required by these rules and principles.*"

Abdulrahman Faaiq Dawood AL-BADRY

ABSTRACT

M. Sc. Thesis

STUDY OF THE EFFECT OF SOME TYPES OF NUCLEAR RADIATION ON SOME PHYSICAL PROPERTIES OF THE TIN OXIDE FILM

Abdulrahman Faaiq Dawood AL-BADRY

Karabuk University
Institute of Graduate Programs
Department of Physics

Thesis advisor
Assist. Prof. Dr. Khalid Hadi Mahdi AAL-SHABEEB
February 2024, 80 pages

In this research, thin films of pure tin oxide (SnO_2) prepared by the thermal evaporation method in a vacuum. We used this method because it is one of the best ways to obtain pure, thin films free of impurities, as the purity rate reached 99% and the impurity percentage was 1 %. Some of these thin films were studied without irradiation, the other was irradiated with gamma rays emitted from cobalt-60 (3.14 and 6.24 rad), and with (thermal and fast) neutrons emitted by ^{241}Am-^{9}Be source $3.05 \times 10^{10}, 6.09 \times 10^{10}$ rad.

The optical properties of these films studied using an ultraviolet device absorbance, transmittance, absorption coefficient, and energy gap before and after irradiation. The results showed that the absorption shift of thin film irradiated for 7 days is less than 14 days, and the behavior is the same as that of non-irradiated thin film.

Measurements of transmittance in the wavelength range from 190 to 1100 nm done for all non-irradiated and irradiated films. The results of transmittance increase with a quasi-stable gradient starting from a wavelength of 191 nm This behavior is identical to the behavior of the transmittance curve in the transparent conductive oxide aggregate, where the transmittance increases rapidly at the cutting-edge region, which confirms the energy gap thin films are of direct type.

Absorbance has the inverse behavior as for the transparent. The absorbance increases for the non-irradiated thin film, reaching its peak at 315 nm and then decreasing afterward. As for the thin film irradiated with gamma, it reduces the absorbance of the thin film, as for the thin film irradiated with neutrons, there was an increase in absorbance. The energy gap is a slight difference between the irradiated and non-irradiated thin films, as after irradiation the energy gap of the thin film decreased.

As for reflectivity, it has the same properties as absorption the electrical properties of the thin film studied by getting the relationship between current and voltage, which is an almost ohmic relationship for the film without irradiation. When the thin film was irradiated, the thin films were very affected, as we find that the breakdown voltage (large response) at voltages ranging between 410 – 988 V for all films, and the films irradiated with thermal neutrons get the most effect, and some of them showed low response.

The structural properties showed by the XRD results of the non-irradiated film growth of four crystalline directions, of which 101 were prevalent. This corresponds to the global ASTM examination card. When the irradiation increases (gamma or neutrons), the peaks disappear because of the transformation of the matter from polycrystalline to non-crystalline.

Keywords **:** Study of the effect of some types of nuclear radiation on some physical properties of a tin oxide film.

Science Code : 20216

ÖZET

Yüksek Lisans Tezi

BAZI NÜKLEER RADYASYON TÜRLERİNİN KALAY OKSİT FİLMİNİN BAZI FİZİKSEL ÖZELLİKLERİ ÜZERİNDEKİ ETKİSİNİN ÇALIŞMASI

Abdulrahman Faaiq Dawood AL-BADRY

Karabük Üniversitesi
Lisansüstü Eğitim Enstitüsü
Fizik Anabilim Dalı

Tez Danışmanı:
Dr. Öğr. Üyesi Khalid Hadi Mahdi AAL-SHABEEB
Şubat 2024, 80 sayfa

Bu araştırmada, saf kalay oksit (SnO_2) ince filmleri vakum ortamında termal buharlaşma yöntemi kullanılarak hazırlandı. Bu yöntemi kullanmamızın nedeni, saf, impuritesiz ince filmler elde etmenin en iyi yollarından biri olmasıdır; saflık oranı %99'a ulaşmış ve kirlilik yüzdesi %1 olmuştur. Bu ince filmlerin bir kısmı ışınlama olmadan incelenirken, diğerleri kobalt-60 tarafından yayılan gama ışınları (3.14 ve 6.24 rad) ve ^{241}Am-^{9}Be kaynağından yayılan (termal ve hızlı) nötronlar ile ışınlandı $3.05 \times 10^{10}, 6.09 \times 10^{10}\ rad$

Bu filmlerin optik özellikleri, ışınlama öncesi ve sonrasında ultraviyole cihazı kullanılarak (absorban, transmittans, absorbsiyon katsayısı ve enerji aralığı) incelendi. Sonuçlar, 7 gün boyunca ışınlanan ince filmin absorpsiyon kaymasının 14 günkünden daha az olduğunu ve davranışının ışınlanmamış ince filmle aynı. Olduğunu gösterdi.

190 ila 1100 nm aralığında dalga boyunda transmittans ölçümleri, tüm ışınlanmamış ve ışınlanmış filmler için gerçekleştirildi. Sonuçlar, dalga boyu 191 nm'den başlayarak neredeyse istikrarlı bir eğriyle artan transmittansı gösterdi. Bu davranış, transmittans eğrisinin saydam iletken oksit birleşimindeki davranışına benzer; burada transmittans, keskin kenar bölgesinde hızla artar, bu da ince filmlerin enerji boşluğunun doğrudan tip olduğunu doğrular.

Absorbansta saydam olanla ters davranış gösterir. Işınlı olmayan ince filmde absorban artar, 315 nm'de zirveye ulaşır ve ardından azalır. Gama ışını ile ışınlanan ince film, absorbanı azaltırken, nötronlarla ışınlanan ince filmde absorban artışı gözlemlendi. Enerji boşluğu, ışınlanmış ve ışınlanmamış ince filmler arasında hafif bir fark olarak ortaya çıkar; çünkü ışınlanmadan sonra ince filmin enerji boşluğu azalmıştır yansıma için ise absorbsiyonla aynı özelliklere sahiptir.

İnce filmin elektriksel özellikleri, akım ve voltaj arasındaki ilişki üzerinden incelendi; ışınlamayan filmler için neredeyse ohmik bir ilişki gösterir. İnce film ışınlandığında, filmler oldukça etkilendi ve tüm filmler için voltaj aralığında 410 - 988 V büyük bir yanıt olan bozulma voltajını bulduk. Termal nötronlarla ışınlanan filmler en fazla etkilenenlerdi ve bazıları düşük yanıt gösterdi.

Yapısal özellikler, X-ışını difraksiyon (XRD) sonuçları tarafından gösterilmiştir. Işınlamayan filmde dört kristalin yönlendirilmesi, bunların içinde (101)'in baskın olduğu görüldü. Bu, küresel ASTM inceleme kartıyla uyumludur. Işınlama arttıkça (gama veya nötronlar), pikler polikristalin yapıdan monokristalin yapıya dönüşüm nedeniyle kaybolmuştur.

Anahtar Kelimeler **:** Bazı nükleer radyasyon türlerinin oksit filmindeki ta'nın bazı fiziksel özelliklerine etkisinin incelenmesi.

Bilim Kodu **:** 20216

ACKNOWLEDGMENTS

To... the beacon of knowledge that taught the educated, the best of beings, my master and my intercessor, the master of creation and messengers, our master Muhammad (may allah bless him and grant him peace)

I extend my thanks to Karabük University and all those who contributed to its development.

I want to thank Dr. Khalid and the doctors of the Physics Department for their efforts.

I also thank Dr. Haider at the University of Baghdad for helping me.

I would like to thank my beloved family for the psychological and moral help they provided me.

I also extend my thanks to the doctors at Tikrit University for helping me (Dr. Kawkab and Dr. Abdullah)

I also extend my thanks to my friends who supported me in times of adversity.

("Thus, work was supported by the Research Fund of the Karabuk University Project)

CONTENT

Page

Page

Page

LIST OF FIGURES

Page

Page

LIST OF TABLES

Page

LIST OF ABBREVIATIONS

ω : Tri phasic tilt

d_{hkl} : The interstitial distance of the group of levels

n : Correct numbers

Q_B : High voltage barrier

(ß) : Curved mid-apex with a system of radii page

G.S : Particle size rate

Eg^{opt} : Blocked energy gap

Hυ : Photon energy

I : Intensity of the transmitted radiation

$I_\circ$: The intensity of the incident radiation

I_A : The intensity of the absorbed radiation

Hυ : The wave function

(α) : Condition is the absorption coefficient.

I_R : Part of the light reflected.

$e^{-\alpha t}$: Monochromatic analysis

r : A constant whose value depends on the type of transitions.

C : The speed of light in a graph

$\lambda_{cut\ off}$: Cutoff wavelength

δ : The phase is a face-centered cube

μ_n : Vacuole movement

σ_{dc} : Continuous electrical conductivity

R : The electrical resistance of the thin film is practically

Å : The cross-sectional area of the electrons moving through the thin film

E_a : The activation energy for electrical conductivity

t : Absolute temperature

σ_o : A constant representing the lowest metallic conductivity

R : An exponential constant whose value depends on the nature of the transitions

(B_Z) : Magnetic field

J_x : Electric current density

Ne : Electric concentration

σ : The conductivity of the thin film

φ_B : An ideal factor is the barrier height

I_{so} : Reverse saturation current

A_{sh} : Schottky contact area

A* : Richardson's effective constant

V_F : Forward bias effort

I_F : Forward bias current

I_{F2} : Forward stream in the tunnel area

I_{S2} : Saturation current in the first region

Ra" : Resistance in the presence of air

Rg : Resistance in the presence of gas

σ_a : The conductivity of the thin film in the presence of air

σ_g : The conductivity of the thin film in the presence of gas

S_{gas} : Thin film sensitivity to gas

S_{air} : Thin film sensitivity to air

Ps : Radiation power

D^* : Qualitative detector

A_D : Detector space

I_{ph} : The output current generated by the lighting

η : Quantitative efficiency

$N_{photons}$: Incident photons absorbed

$N_{carriers}$: Number of photo generated

I_s : It is at reverse bias and is the saturation current

(I_{th}) : Thermal noise current

K_B : Boltzmann constant

I_{sn} : Injected carriers

R_{λ} : Spectral response

I_d : Dark stream

I_N : Noise stream

C_o : The capacitance of the depletion region

$t_{response}$: Response time

τ_{rise} : Life span of carriers

AFM : Atomic force microscope

XRD : X-ray diffraction

FWHM : Width of the middle of the curve at greatest intensity

PART 1

INTRODUCTION

In this chapter, we will talk about thin films and their access to modern technologies such as nanotechnology. The thin films are a branch of material science in physics, and they measured in very small units, such as nanometers. It is widely used in modern technology and solar cells and the resulting ions have different and important properties [1] [2].

There are many step, we must follow before depositing films. We choose the materials according to the study we need, and we choose the appropriate base on which we will deposit the material so that it does not interact with it. The samples examined with some devices and the thickness of the thin layer detected with the device designated for it [3].

Due to its importance and the different methods of manufacturing and preparing it at different levels and types, and due to its small size, ease of manufacture, and low cost of production, it entered small electronic devices such as computers [4].

Heterojunction is one of the applications of thin films produced from semiconducting materials, and the two materials must be different from each other. This idea was proposed by (Williamn Shokiley), in 1951 for the first time, and because of this idea, it was used in water sterilization, and also in military applications [5] [6].

The use of modern, low-pollution technologies will reduce the emission of gases that lead to global warming and the possibility of fuel expiration in the coming years. This is the reason that prompted a group of scientists to search for modern technology to consume clean energy and at the same time be cheap, and this is one of the reasons for reducing the consumption of natural resources where they were able to convert wind energy into electrical energy and also convert light energy into electrical energy[7] [8].

In 2014, the consumption of light energy was measured, as the investment of light energy for citizens and companies was 53.3 %, ranging between 35 gigawatts and 42 gigawatts, compared to the year 2012. The light energy was invested by 14 % [9] [10].

Nanotechnology entered into solar cells due to their small size and high efficiency, and it is transparent and cheap, as nanotechnology helps in photon absorption[11].

Scientists have been able to manufacture the nanoscale shapes that exist in this era, such as optical cables, nanofibers, and high-conductor transistors, and also manufacture nanowires. The manufacturing of these things is linked to several departments, including the thin film department. [12].

1.1. THIN FILM

The methods used in the preparation of thin films are many, and each method differs according to the type of material used, temperature, manufacturing cost, intended purpose, and purity, it has several applications, including chemical and physical applications, and as we see here some types of preparation method of thin films[13].

- Chemical Spray Pyrolysis
- Chemical Vapor Deposition
- Electrodeposition
- Sol-Gel
- Reactive Magnetron Sputtering
- Thermal Evaporation under Vacuum
- Molecular beam epitaxy
- Spin Coating
- Pulsed Laser Deposition (PLD)
- Thermal oxidation

Thermal Evaporation under Vacuum method has been used in this research because it is one of the best methods to obtain high purity and we must not forget

nanotechnology, as it is directly linked with semiconductors, and its thickness ends at 1 nm and starts at less than $100nm$, and its manufacture is associated with thin films.

Thin films are involved in the manufacture of solar cells, and their working mechanism to produce electrical energy is when we expose the cell to light. Through this process, a potential difference and electricity will be produce. But there are conditions for producing electricity, including that the electron must move from the solar cell to outside the solar cell, and the condition of this electron is that it has the highest energy, as it returns to the inner circle after losing its energy in the outer shell.

1.2. THERMAL EVAPORATION IN VACUUM

It is one of the best techniques that we use to obtain high purity, as it is easy to prepare and also has a cheap cost, and these advantages help to use this method in abundance and less damage to the material to be worked on, as well as less damage to the surface to be sprayed on. Also less damage to the device, as the spraying process takes place inside a chamber under pressure and the pollution process inside the chamber is very rare and we use the pressure inside the chamber to reduce the collision between the air atoms present inside the chamber and the atoms to be worked on. Heat will separate compounds from each other, and this method is not good for preparing thin-film minerals as we can see in figure 1.1 [14] [15].

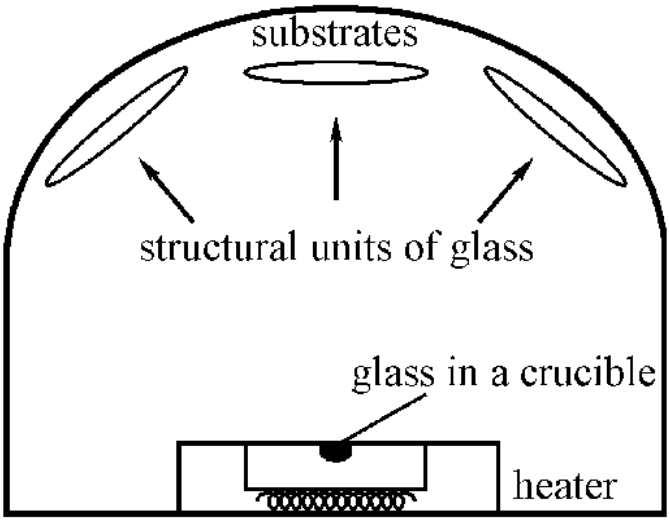

Figure 0.1. Thermal evaporation chamber [16].

We can summarize the preparation process by placing the material to be work on inside the chamber, where the basin is made of molybdenum or tungsten. Where its melting point is very high, higher than the material to be work on, the material placed in the device. According to the desired thickness two pumps are connected. The first is mechanical. This pump reaches 10^{-3} Torr, and the second pump will reduce the pressure to 10^{-7} Torr meanwhile, the temperature rises, and a thin layer is formed when the substance evaporates. It collides with the floors that we previously placed and their temperatures will gradually decrease.[17] [18].

As previously mentioned, thin films are directly involved in the creation of nanomaterials because there are several ways to prepare them. The first method is bottom-up, in which the material's particles form an orderly structure; this method differs from the others in that it is chemical rather than physical. The second method is top-down, in which we smash the original material smashing techniques. Many of them are grinding and cutting, and in these ways, they reach nanoscale size, and we benefit from them in various microelectronic devices. As we will see in the following table, the extent of the importance of the thin film [19].

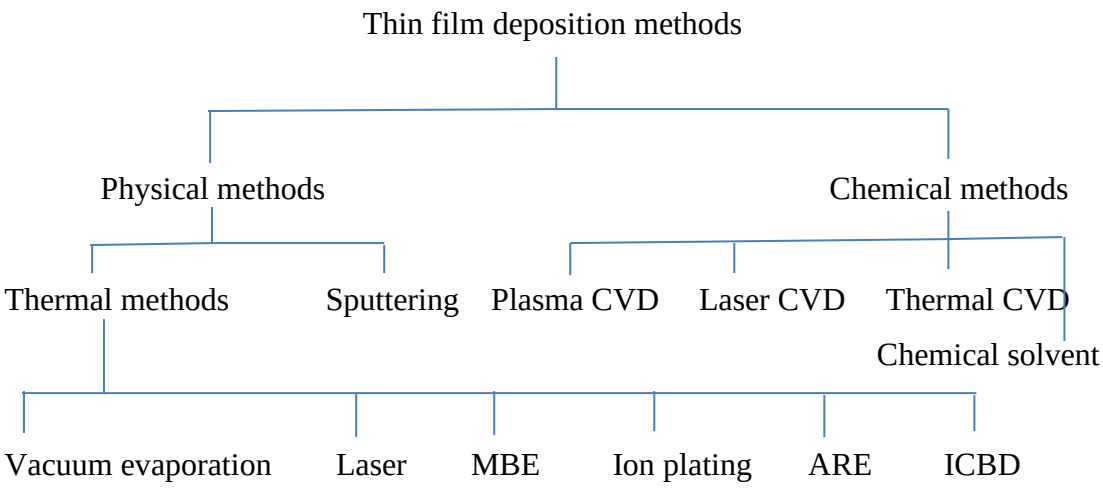

Figure 0.2. Diagram different deposition techniques for thin films [20].

The following figure shows the importance of thin films and their connection to other sciences.

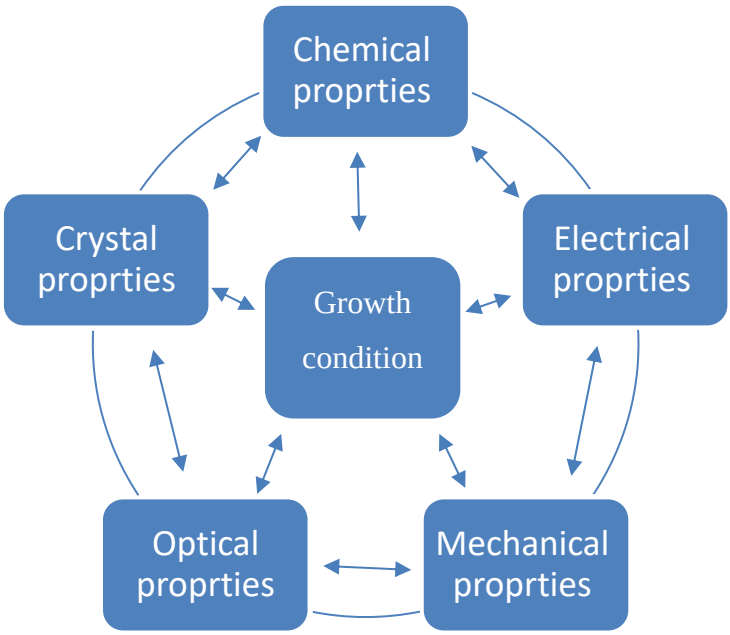

Figure 0.3. Thin films connection to science.

1.3. THIN FILM'S RELATIONSHIP WITH RAYS

This study aims to improve the relationship between thin films and the irradiation process, study the radiation effect on optical and electrical properties and the crystal structure of SnO_2 film the film, and study the results before and after irradiation.

The term "radiation" refers to atomic alterations that occur spontaneously and emit energy, including atomic nuclei. These modifications result in the discharge of energy as electromagnetic radiation or particles that interact with the medium to varying degrees [21].

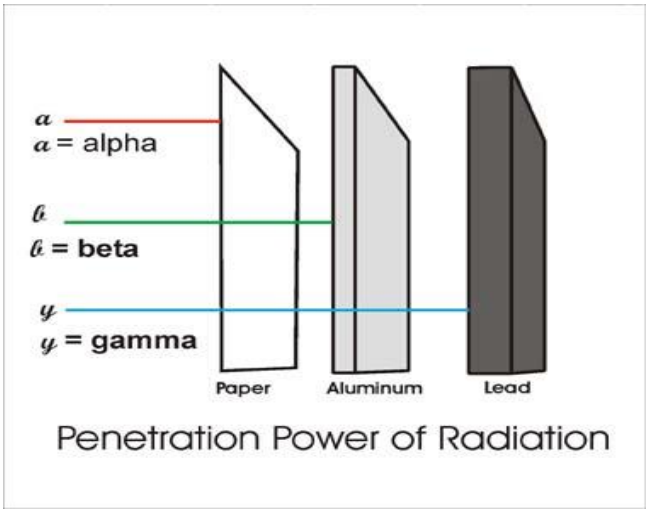

Figure 0.4. Types of rays and their penetration into the body [22].

The term "radioactivity" refers to the process of an isotope's nucleus spontaneously decaying into a smaller nucleus or a nucleus with a lower energy value while emitting particles, which involves the emission of one or more photons or gamma rays. Depending on the process's nature and the physical characteristics of the nucleus's condition both before and after breakdown, it might occur or it might not [23].

1.4. RADIOACTIVITY UNIT

- Curie: Its value is equal to 3.7×10^{10} dis, and it is a conventional unit of radiation measurement and emits from (226Ra) per gram.
- Becquerel: Decay per second is equal to (B_q) in Curie equals to 3.7×10^{10} Becquerel.

Radiation is divided into two types, ionizing, and non-ionizing.

Ionizing: alpha particles, beta particles, X-ray gamma rays, protons, neutrons non-ionizing radiation: visible rays, infrared, ultraviolet, radio waves, and microwave types of radiation dose

- The absorbed dose is defined as the amount of energy absorbed in joules per unit mass of the substance in kilograms and can be written mathematically as follows: $\mathrm{D} = \mathrm{E}/\mathrm{m}(\mathrm{J}/\mathrm{Kg})$
- The equivalent dose H_{ti} is defined as the product of multiplying the absorbed dose, D_{ti}, by the weighted radiation coefficient, the specificity coefficient:

- $\mathrm{H_{ti}} = \mathrm{D_{ti}}\ \mathrm{x}\ \mathrm{W_R}$

- The Effective Dose (E_{ti}): The whole-body effective dose E is the sum of the equivalent doses. The weighted radiation factor is multiplied by the tissue weight factor and is determined according to the equation: $E = \sum \mathrm{Wti}\ .\mathrm{ti}$

PART 2

PREVIOUS STUDIES

The optical and electrical properties of the SnO_2 thin film after treatment using cold plasma were studied by Abdel Amir in (2017). The dielectric constant ε and optical conductivity σ were calculated. It was found that increasing the exposure time to plasma reduces the extinction coefficient and the refractive index, which leads to an increase in optical conductivity, in addition to a decrease in the dielectric constant with an increase in the exposure period to cold plasma, this thin film was prepared by chemical spray pyrolysis [24].

In (2013), Sabri Wathaer prepared the SnO_2 thin film by thermal evaporation in a vacuum and then studied the structural properties using XRD. They found that the thin film was polycrystalline and of the quadrilateral type. An AFM test was also carried out to show that the thin film was nanotype. Optical tests were also carried out to measure the transmittance for the wavelength range of $300 - 1100$ nm, which has a maximum value of 85 % in the visible light range. The optical energy gap was also calculated and was 2.990-volt direct transmission allowed [25].

The researchers, Battal and Duskan 2019, deposited thin films of SnO_2 film doped with antimony and fluorine on glass using the spray pyrolysis technique. They showed the effect of the spray temperature on the optical and structural properties of the film. The average purity was about 83 %, and the optical energy gap changed with the temperature change, which ranged from 3.10 to 3.89 volts. As for the structure of the thin film, it was multiple, and its directions were 1 0 1, 2 0 0, and 2 1 0 for all temperatures. The SEM and AFM gaps also confirmed that the surface of the thin film was homogeneous, that it was affected by changing temperatures of the substrate, and that it was of the nano type [26].

In (2019), researchers Elias and Al-Dulaimi used the chemical vapor deposition technique under normal atmospheric pressure, (APCVD), to prepare the first undoped SnO_2 thin film and the second SnO_2 doped antimony thin film with different concentrations of 1-1.4 at a temperature of 480 ℃ for study the optical properties of the grafted and non-grafted thin films. The results indicated an increase in reflectivity and refractive index with an increase in the concentration of antimony grafting and a decrease in the rate of transmittance with an increase in the concentration of antimony. As for the absorbance, absorption coefficient, and deactivation coefficient, they increased with an increase in the concentration of antimony, while the energy gap changed slightly during the grafting process. It was shown that these effects are due to vaccination [27].

Sayyed and others (2022) prepared samples of the tin oxide SnO_2 and determined their effect of percentage presence on the optical and radiation attenuation in the stimulated films to make glasses for the radiation field in the films prepared at1100 ℃. They are calculating the optical properties of the glasses irradiated by a beam of ultraviolet and infrared rays close to the visible spectrum that is with a wavelength rang200 and 3000 nm. The shilling power to the γ-rays with an energy range between 0.244 and 2.306 MeV was calculated by performing simulations of the models prepared using the X.COM program, and its results for linear attenuation were good, which increased with the addition of SnO_2. This was observed at an energy of 0.244 MeV, so the linear attenuation was $0.389\ cm^{-1}$ [28].

Kayed and others (2003) developed a method to obtain a homogeneous layer of CnO_2 by using a low-scattered CO_2 laser of 70 watts continuously, and under normal atmospheric pressure by vaporizing targets made of tin oxide. Then annealing these films to study the optical, structural, and electrical properties to demonstrate the effect of heat annealing on these properties, and the results indicate that the intense heat treatment with the resulting roughness leads to enhancing the orientation of the crystalline orientations according to the 110 planes. It also leads to a change in the energy gap and its value. The technique used to obtain this thin film has applications of importance in the fields of superconductivity, solar cells, optical sensors, and materials with electrical stress [29].

Latif in (2012) presented research to the international atomic energy agency on the effect of gamma rays on the physical properties of the creation of miniature SnO_2 by the method of thermochemical spraying and a concentration of 0.1 M, with a base temperature of 400 °C and two thicknesses of 175 and 300 nm. The optical properties of this thin film were measured at visible and near-infrared wavelengths, which included transmittance, absorbance, absorption coefficient, and energy gap before and after irradiation with gamma rays. The results showed an increase in the value of transmittance and the optical energy gap with increasing irradiation doses. The thin films were irradiated with two courses: ^{137}Cs which has an energy of 0.62 MeV, and ^{60}Co, which has an energy of 1.173 MeV and 1.332 MeV for 14 days.

In (2012), Nour et al. worked on the preparation of undoped zinc oxide films doped with tin Sn on glass bases using the method of thermochemical analysis at a temperature of 450 °C and a concentration of 0.1 ml and a spray rate of 10 ml per minute. Different distortions were found, so the thickness of the films was about 400 nm. When film conducting, the necessary tests for the study, optical lead In the synthesis, it was found that the repulsive increased with an increase in the percentage of doping with tin, the highest value was 79 % and that the optical energy gap allowed for direct transmission for the doped films was 3.43 eV and that for the undoped films was 3.25 eV, while the Auerbach energy was concerned with an increase in the percentage of doping and was 291 MeV with the highest doping and 455 MeV for the undoped films. The extinction index, refractive index, optical properties, and other properties were calculated as a function of photon energy. However, X-ray examinations only show that the structure of these films and the crystallinity are of the hexagonal type, and the prevailing trend is 002 for the doped films, this trend has decreased [79].

Aqlo (2018) studied the effect of neutrons on the optical and structural properties of MnS films prepared by thermal discharge at room temperature of 27 °C. They were 400 nm thick and had a deposition rate of 10.39 nm/s on a glass slide. These films irradiated with a neutron source ^{241}Am-^{9}Be with flux of $3 \times 10^5 \mathrm{n/cm^2.s}$ for a period of one and two weeks, optical tests were conducted that included transmittance, reflectivity, and optical energy gap, in addition to X-ray diffraction examination. These

change in this thin film become possible to use in optical detectors and sensors espially in medicine field [30].

In (2005), Haboubi and other researchers studied the effect of gamma rays on the optical properties of SnO_2 and SnO_2 films prepared using the thermal deposition technique and irradiated with ^{60}Co source with an energy of $1.173\ MeV$ and $1.332\ MeV$ for three hours at a distance of $10\ cm$. The results indicate that the optical constants, such as absorption, reflectivity, extinction coefficient, and refractive index, decreased with increasing of the irradiation period, in addition to the fact that the optical energy gap decreased with the increase in the percentage of doping with the aluminum material, compared to these values for the thin film before the gamma ray irradiation process [31].

In (2020), researchers Adriama and others studied the optical, structural, and morphological properties of a fluorinated tin oxide (FTO) film for use as a thermal coating around small future spacecraft. The films were prepared with a high density $2.5 g/cm^3$ and a surface electrical resistance $12\ \Omega\ sq^{-1}$ with a thickness of$450\ nm$. These films irradiated with a ^{60}Co source with two energies 1.173 and$1.332\ MeV$, for different exposure time to obtain doses of 20, 30, and$50\ Gy$. The X-ray diffraction and AFM examination revealed that there is an evolution in the structural properties as a result of enhanced crystallization after irradiation, in addition to a change in the size of the crystals with an increase in the dose, that reduced surface roughness and a difference in optical transmittance of (FTO) films was observed [31].

Majeed et al. (2015) studied the optical and electrical properties, in addition to the structural properties of the SnO_2 Nano-thin films for dye-sensitive solar- cells. They concluded that radiation led to a deterioration in the performance of the SnO_2 Nano-thin films as result of the change caused by the radiation in the structure of this thin film, which led to an increase in the refractive index. The radiation dose increases in the optical energy gap to $3.95\ V$ at a dose of $6\ kGy$. The specific resistance of the film decreases after the irradiation process also decreased by $40\ \%$ at $659\ nm$, which led to an increase in the movement and concentration of the carriers [32].

In another study at (2021) done by Al-Baradi and others, they conducted the effect of gamma rays with doses of 50 to 200 kGy on the microstructure and optical properties of the SnO_2 thin film. The results showed a slight increase in the crystalline size of the film with an increase in the dose, which led to a change in the permissible optical energy gaps [33].

In a recent study in (2023), conducted by Kajal and others, to study the effect of gamma rays with doses of 75, 100, 125, and 200 Gray on the structural, morphological, optical, and electrical properties of the SnO_2 thin film. The fact is that gamma rays are electromagnetic rays. That work to change the crystalline structure of the thin film and that shown in XRD results of the thin film. Where the crystalline size increased to 49.27 nm due to the increase in the radiation dose, while the energy gaps decreased from 3.8 to3.4 eV, as the Raman spectra showed the presence of defects as result of irradiation. These semiconductor thin films appears to lack properties: i.e. an increase in electrical conductivity at the low dose of 125 kGy and decrease to 200 kGy. The researchers concluded that irradiation can modify the properties of materials such as thin films for the purpose of using them in sensing and radiation detecting operations [34].

PART 3

THIN FILMS

In this chapter, we will discuss the equations of thin films, their electrical, structural, and optical properties, how they exist in nature, and their crystalline structures.

3.1. SEMICONDUCTORS

The use of thin films in accurate devices indicates that they can conduct electricity, and there is a difference between the doped and the undoped thin film, as the doped film cannot withstand high temperatures, high electric current, and pressure, while the pure, on the contrary, can withstand high current, temperature, and pressure.

Semiconductors are also characterised by their ability to electrically insulate, which is one of their advantages [4] [35].

- You can connect the positive pole of the electric current and the negative pole of the electric current
- The electrical resistance decreases in the presence of impurities. The greater the impurities, the lower the resistance in the electrical circuit
- It works to change the acceptor into a donor and the donor into an acceptor [36]
- Each conductor has a resistance, where the resistance of tin oxide ranges between $10^{-3} - 10^{-8}$ $(\mathrm{W.cm^{-1}})$
- Having charge carriers and having gaps
- When exposed to light, a high sensitivity appears, and this exposure called photoelectric.
- Semiconductors are directly proportional to temperature.
- The semiconductor in the Fermi level is of high purity and appears only at low temperatures.

3.2. CLASSIFICATION OF SEMICONDUCTORS

There is a gradation according to the crystalline levels first crystalline semiconductors and there are two of them.

- Monocrystalline: and its atoms are regular, that is, its dimensions are regular and of equal distance between them, and because of this arrangement, the internal energy is low, as in Fig. 3.1b.
- Semiconductors Polycrystalline: many semiconductors have a polycrystalline system, and the electrostatic potential creates a crystalline defect and creates a crystalline barrier, and this barrier delays charge carriers in figure 3.1c [37].

Second - Amorphous Semiconductors: Its unstable thermal system due to the stopping of its atoms in, its place in the process of crystallization, and we cannot reach the state of balance, as in some semiconductors such as silicon, and its range is short, and its crystal system is trying to arrange itself when its internal energy is disappeared. After losing that energy, it returns to its normal state, where the value of the energy is an else we can differentiate between random and crystal materials by examining x-ray and electrical properties, as it appears in one-crystal material that appears the shape of the crystal in the form of points as in figure 3.1a [35] [38].

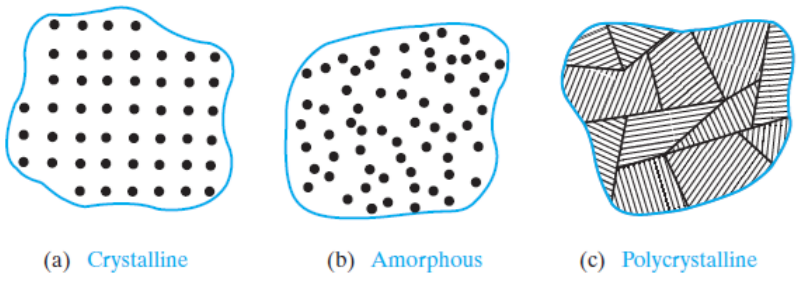

Figure 0.1. Crystal shapes : a- single b- multiple c- random [39].

3.3. ENERGY LEVELS

To calculate the energy levels, the synthetic and visual properties of the solid thin film must be determined it has monatomic electrons and accommodates two electrons, and

each of the electrons spins opposite the other, and is determined by a quantum number n according to the Pauli exclusion rule [40].

And the crystalline energy levels are split up and reach the N level, and they form a group of bundles, in the following figure, will show the equivalence slit where this beam is located after the delivery packet as we can see, energy comes in three forms. Insulating, conductive, and semi-conductive materials, and in insulating materials, the valence bands are high, as energies such as thermal energy cannot raise electrons because they are filled with electrons, and at this level their conduction band is empty. The energy gap is eV $= 9$ Eg, which is greater than the energy gap of conductive materials. and semiconductors as in Figure 3.2 a [40] [41].

The conduction bands in semiconductors are all empty, their energy gap is not the same as in insulators, where its capacitance is less, and the valence band in semiconductors is saturated, and the energy gained by electrons can be transferee to conduction bands using energy gaps, as in Figure 3.2 b.

As for conductors when they gain energy filled with electrons in the valence band to a higher energy band, the current will move more smoothly like in Figure 3.2c [42].

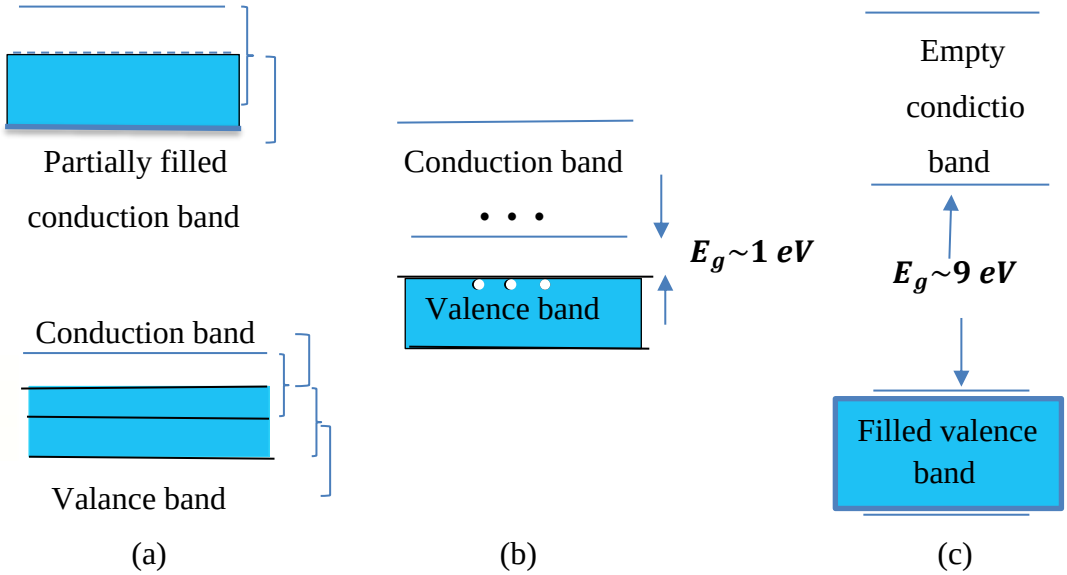

Figure 0.2. Energy bundles [43].

3.4. STRUCTURAL PROPERTIES

There are several properties of thin films, including synthetic, visual, and electrical properties, and we will address them one by one

The synthetic characteristics are one of the characteristics through which we can learn about the quality of the thin thin films procedure and also the physical results and changes that appeared on the thin films after the preparation and also the type of crystal levels and external changes that occurred on the thin film and the nature of the materials used with prohibition and their purity ratio

There are three methods for measuring synthetic properties

1-(XRD) 2-(AFM) 3-(SEM)

3.4.1. X-Ray Diffraction

The X-rays are of high energy and are waves located between two rays, gamma rays, and ultraviolet rays. X-rays are electromagnetic rays and lie within $0.1 - 100$ Å and are of positive lengths [44].

We can study the diffraction of X-rays by projecting rays at a certain angle θ, and these rays are mono wavelength. X-ray diffraction is used to identify crystal shapes, their composition, and whether they are multiple, single, or random[45].

And that the X-ray diffraction peaks are distinct at the preparatory conditions, and the reason for this distinction is the preparatory conditions for the atomic levels, which in turn will reflect the X-rays, and as a result of this work, the reflected rays will produce constructive interference and that Bragg's law is the condition for achieving reflection $1 \leq 2d_{hkl}$ [46].

3.4.2. Bragg's Law

We can calculate the interfacial distance using this law, and its angle must be known for each vertex of θ_B. The law given in the form.

$$n\lambda = d_{hkl} \sin(\theta B) \quad (3.1)$$

where it represents

d_{hkl}: The distance between the levels
n: Correct numbers
l: wavelength of radiation $\lambda_{X_{Ray}} = 1.5406$Å.

To identify some of the crystalline details, we use X-rays, such as the number of crystals in the bound film, the lattice constants, the density of dislocations, and the volumetric rate of the grains we will explain how to calculate the particle size[47].

And we will explain how to calculate the particle size, as the particle size is a factor to know the characteristics of the particle, and the particle size G.S for the blocked films is calculated by the Debye-Sharar equation [47].

$$(G.S) = \frac{0.94\ (\lambda_{X-Ray})}{ß\, cos\theta} \quad (3.2)$$

(ß) : Curved mid-apex with a system of radii
($\lambda_{X\text{-}Ray}$) : X-ray wave 1.5406 Å

The greatest intensity of the curve is at the middle and we can calculate the maximum curve intensity by calculating the middle of the peak, in this case, we will be able to convert from a system of units to a radial system [48].

According to the (Sherr) equation, the size rate is important in determining the properties.

$$CS = \frac{0.94}{\beta \cos\theta} \qquad (3.3)$$

(β) :It is curved with a combination of radial units.

And that the size of the crystal S.C and that the particle is cubic and the size of the particle is measured from $V = C.S^3$ [49] .

3.4.3. Scanning Electron Microscope (FESEM)

Because of its superior degree to all other microscopes and its image created by the three-dimensional microscope, as shown in Figure 3.3, the electron microscope regarded as one of the most significant examination systems of the modern period. Displays all cracks, holes, and scratches, after this scan through an electric field and interaction with the sample's surface, an electron is specifically extracted using a magnetic field. The electrons detected by the electrons that reach the detector, and we can determine that they recorded an electron by using the additional sensors. [50].

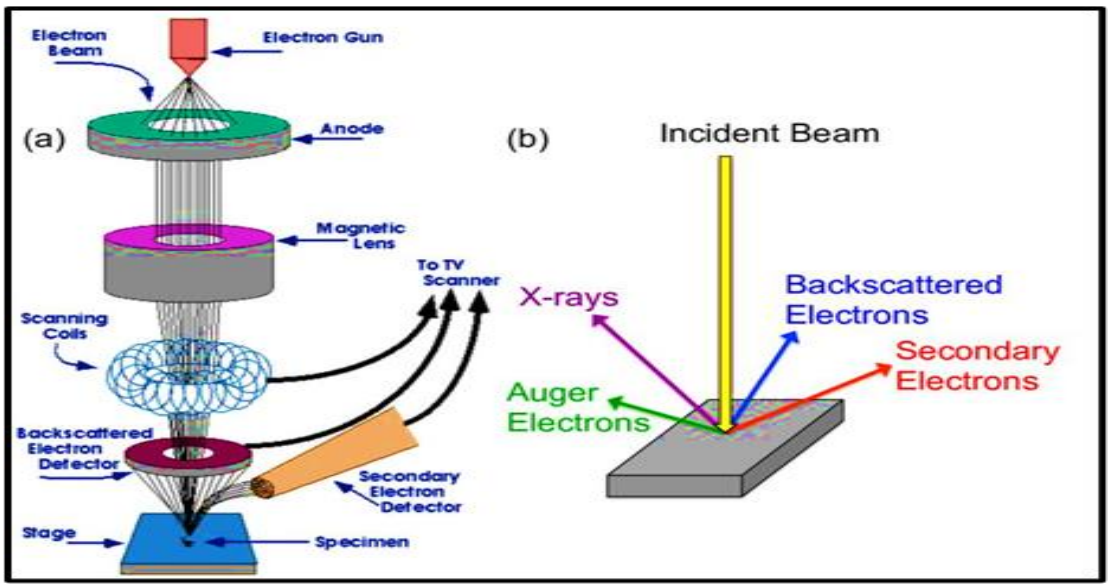

Figure 0.3. Electron microscope and its steps [51].

3.4.4. Energy Dispersive X-Ray Spectroscope (EDS)

One of the tools connected to the SEM, is the energy dispersive spectrometer. Which operation based on identifying the energies of this type of measurement. That is crucial for all elements affected by the electron beam's descent (the membrane and the base) in the form of tables because the high intensity of the falling electrons increases the likelihood that the electrons will uproot the material's core, revealing every element present in the composition—even if it is that represents a very modest percentage[52].

3.4.5. Atomic Force Microscope Measurements (AFM)

Its technology depends on the Scanning Tunneling microscope, which is one of the types of scanning probe microscopes. One of its advantages is its magnification of materials, estimated at 5×10^{2}- 10^{8}, and its high analysis is also estimated at 0.1- 10. It does not need a vacuum chamber like an electron microscope it can work at normal pressure.

A microscope consists of a probe at the end of an arm, and its head used to scan the sample. The material of this arm is silicon nitride Si_3N_4, when the sharp tip of the probe approaches the sample a certain force will be generate between the tip of the sharp probe and the surface of the sample, so the arm deflects due to the force according to Hooke's law. The force may be a mutual mechanical force, Vannervals force, or electrostatic force, and the forces change according to the type of surface.

The model examined after we put it on a moving base according to the principle (Piezoelectric) and controlled in all directions and electronically and the microscope has more than one pattern for operation. The wiping done in the microscope according to the ability to be enlarge by moving the fool on the side of the microscope. The detector will feel the reflection of the laser, which will happen when the wander deviates and the reflection repelled by the detector. We describe it linearly and when the detector moves it will produce a movement and this movement is the terrain. That wiped in the sample and whose curvatures and deviations examined and this terrain drawn through the computer figure 3.4. When we want to measure the surface of the

insulation the semi-insulators and connectors use (AFM), which gives us information about the surface of the sample, such as the number granules and the roughness [53].

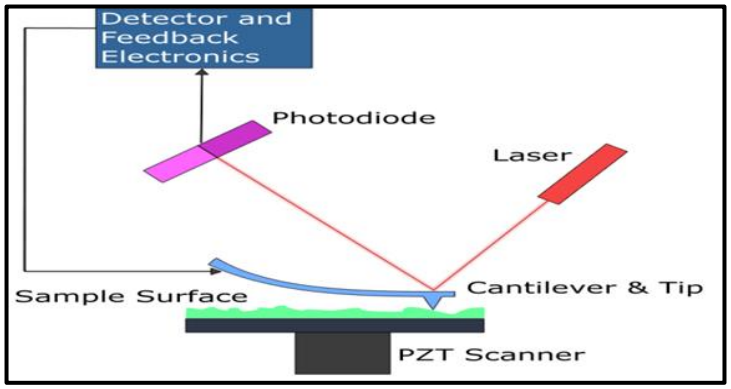

Figure 0.4. Atomic power [53].

3.4.6. Fourier Transform Infrared (FTIR)

One of the electromagnetic waves that generated from particles and hot bodies, and for these we use infrared waves. The infrared energy absorbed by a group of objects appear in the form of heat, because of the thermal energy gained by atoms, where these atoms increase the vibrational movement, then the temperature rises. The visible rays come first, and after that the infrared rays, and before that comes the region that affects the level of rotation and the vibrational energy of the particles together and is divided into [54].

- Far infrared and range between 200-10 cm^{-1}
- Central infrared range between 4000-200 cm^{-1}
- Infrared range between 1200-4000 cm^{-1}

Infrared technology is one of the means, which we can see the changes in rotational and vibrational energies - the rotational motion the absorption of molecules, and the emission of molecules resulting from movements, and it has a moment in the infrared rang, and through it, it can absorb light and emit light whose frequency is less than 250 cm^{-1}. The particles that absorb energy due to the rotational movement and in the region $200 - 3500\ cm^{-1}$ appear I bundle.

And if we use (FTIR) instant analyses of infrared radiation, the study was, limited to studying nanostructures and absorption bands, and in the following equation, which is a basic equation for studying molecular vibrations [55].

$$\nu = \frac{1}{2\Pi c} \cdot \sqrt{\frac{k}{\mu}} \tag{3.4}$$

ν: wave number, μ: reduced mass, k: Fixed bond strength3.5.

3.5. OPTICAL PROPERTIES

It is important to study the optical properties so that we can learn about semiconductors in terms of electronic transitions, the energy gap (E_g), the absorption coefficient, and the study of other optical constants systems.

When we shine a light on the thin film, the film will absorb part of the light that focused on it, and this part of the property called optical absorption, as the incident light will lose part of it as a result the interaction of the incident photons with the electrons in the material.

The interaction between matter charges and the electric field accompanying electromagnetic radiation leads to the emergence of a spectrum of matter absorption and optical properties [56] .

Valence band in the ideal semiconductor, the conduction band is empty, and, the valence band is filled with electrons, and the electrons themselves cannot move from the valence band to the conduction band, when we apply the energy of its photons hν equal to or greater than the forbidden $EG \geq E_g$, and in the semiconductor this energy is capable of creating a pair electron-gap, and that the electrons the valence band to the conduction band after they absorb the light energy of the incoming photons, creating optical conduction as in the following [56] [57].

The energy of the photons falls in a state equal to a pure semiconductor with the ratio of the forbidden energy gap, that is, $hv = E_g$ as in the previous the incident radiation $V_\circ$ whose frequency called the threshold frequency. And the fall of photons produces an increase, and this causes rapid absorption, as this part of the work is called the absorption edge [58].

If the forbidden energy gap is less than the energy of the incident photon ($hv > E_g$) there is a difference in excess power $hv - E_g$. This energy will be lost in the form of heat energy, and if the E_g of pure semiconductor is higher than the energy of the photon. The photon penetrates the semiconductor and is not absorbed , the photon penetrates Semiconductor and is not absorbed, but enters through the semiconductor , and that electronic transitions do not occur in pure semiconductor, but electronic transitions occur in doped semiconductor, and that is the forbidden energy gap E_g of impurity levels as [59].

Transition and the transition called a self-transition, or it called a transition from a beam to a beam, and the last transition is a non-self-transition and does not occur due to the presence of energy in the prepared gap, which produced by chemical impurities as well as physical defects in the pure semiconductor.

3.5.1. Transmittance

The symbol for transmittance is T, it is defined as the intensity of the transmitted radiation I relative to the intensity of the incident electromagnetic radiation I_0 and the permeability is free from any units of measurement it does not have any units.

$$T = \frac{I}{I_o} \tag{3.5}$$

(T): The transmittance that dependence on

- Thickness: the lower the thickness, the higher the permeability.

- Staining ratios: the inoculation increases the permeability or decreases the permeability, and in previous research, we see a reverse process that reduces the permeability, and this thing caused by an increase in the objective levels, so the absorbance ratio increases over the permeability.
- Preparation method, temperature, and other conditions[55].

3.5.2. Absorbance

The absorption process takes place inside or outside the model that we made, and A is defined as the ratio of the radiation absorbed by the thin film I_A to the radiation falling on it I_0, as in the previous and it is free of unis, as we can see in the following relationship [60].

$$A = \frac{I_A}{I_o} \tag{3.6}$$

The relationship between transmittance and its connection with absorbance is as we can see in the following relationship[61].

$$A = Log_{10}\left(\frac{1}{T}\right) \tag{3.7}$$

$$\therefore\ T = e^{-2.303A}$$

3.5.3. Absorption Coefficient

As a part of our calculations for thin films, we must find α an absorption coefficient, and we can calculate photodetectors and cell designs the absorption coefficient is defined as the system of decreasing incident radiation flux per unit wave propagation distance [62].

With different materials, the wave functions hυ the radiation falling on the thin films with the Optical energy gap(E_g), and the solar cells directly affect it, as it absorbs part of the light, this condition is called the absorption coefficient(α).

When part of the light beam $I_\circ$ falls on the prepared thin film, part of the radiation penetrates the thin film I and part of the light is reflected I_R, and there is part of the light is absorbed by the thin film I_A, as in the previous.

The range of penetrating, reflected, and absorbed energies all depends on the nature of the thin films and the wavelength of the incident light λ, as well as α denotes the absorption coefficient and its ability to absorb the incident radiation [60].

This is a physical phenomenon, as it passes through a semiconductor with which the monochromatic decays exponentially $e^{-\alpha t}$, and according to the following equation, the intensity of light $I_\circ$ over the thickness of the material t and the absorption coefficient α, the light intensity I we will use the Lambert absorption coefficient [63].

$$I = I_o \, e^{-\alpha \, t} \tag{3.8}$$

We can write the equation in the form.

$$Ln\left(\frac{I}{I_o}\right) = -\alpha \, t \tag{3.9}$$

By solving this equation, we get

$$\alpha \, t \; = \; 2.303 \, \mathrm{Log}_{10}\left(\frac{I}{I_o}\right) \tag{3.10}$$

Since $\{\mathrm{Log}_{10}\left(\frac{I}{I_o}\right)\}$ where represents the absorbance A, in the thin film, and according to the 3.10 equation we will get the following absorption equation.

$$\alpha = (2.303) \; \frac{A}{t} \tag{3.11}$$

(α): Absorption coefficient, his loneliness cm^{-1}

(A): Thin film absorbance

(t): Thin film thickness measured by cm.

3.6. FUNDAMENTAL ABSORPTION EDGE

When the energy of the incident radiation photons hν is approximately equal to the energy of the prepared gap (E_g), a rapid increase in absorption occurs. This known as the fundamental absorption edge and it corresponds to the lowest energy difference between the highest point in the valence band and the lowest point in the conduction band.

All semiconductor materials will quickly and sharply absorb incident light, but this property is only present in monocrystalline materials; It is less pronounced in polycrystalline semiconductors [63][64].

Wave $\lambda_{\text{cut ff}}$ is calculated.

$$\because \ (\text{hv})_{\text{photon}} = \text{E}_\text{g} = \frac{\text{h c}}{\lambda_{\text{cut off}}} \tag{3.12}$$

(h): Planck's constant $\text{h} = 6.626\text{x}10^{-34}\text{J.sec}$
(c): The speed of light in a vacuum, Compensation in constants produces.

$$\therefore \ \lambda_{cut\ off}(nm) = \frac{1240}{E_g(eV)} \tag{3.13}$$

The cut-off energy λ_{cutoff} of a pure semiconductor defined as a wavelength and corresponds to the forbidden gap (E_g). Whose value the optical absorption process begins, which reveals the fundamental absorption edge of the semiconductor.

3.7. ABSORPTION REGIONS

It divided into three regions.

First: High Absorption Region: depicts the region where electronic transitions take place from extended levels in the valence bands to extended levels in the conduction

bands and the absorption coefficient α is greater or equal to $10^4 cm^{-1}$. Determine the energy of the blocked optical gap through this region (E_g^{opt}).

Second: Exponential Absorption Region: the value of α in the area ranges from $1cm^{-1} < \alpha < 10^4 cm^{-1}$ they stand for changes from the local levels at the top of the valence band to the extended levels in the conduction band as well as changes from the extended levels in the conduction band to the local levels at the bottom of the valence band.

Third: Weak Absorption Region: showed us that the absorption coefficient is very small $\alpha < 1\ cm^{-1}$, and the area depends on the percentage of the thin films in terms of the impurities in it. The purity, the method of preparing the thin films, the transmission of electrons, and the density of electrons within the movement space, which produces defects in the crystal structure within the energy gap E_g.

3.8. ELECTRONIC TRANSITIONS

The photon falls and the electron absorbs its energy to move from a lower energy level to a higher energy level, which results in the absorption process. The top of the conduction band does not always directly overlie the valence band in semiconductors because the top energy of the conduction band (C.B) may first coincide with the position of the incident electromagnetic wave during these transitions, transferring the electron from the valence band through the forbidden energy gap to the conduction band. When the position of the valence band energy (V.B) and the wave vector space k coincide, it claimed that the semiconductor, such as gallium arsenide, has a direct intrinsic gap GaAs. A semiconductor has an indirect self-gap if the above-mentioned coincidence does not occur, such as silicon Si as in figure 3.5. In semiconductors, electronic transitions are divided into [65] [61].

- Direct transfers, divided into
  - a- Transfers not allowed directly electronically.
  - b- Transfers allowed directly electronically.
- indirect transfers

a- Indirect electronically permitted transfers.

b- Indirect electronic transfers not allowed.

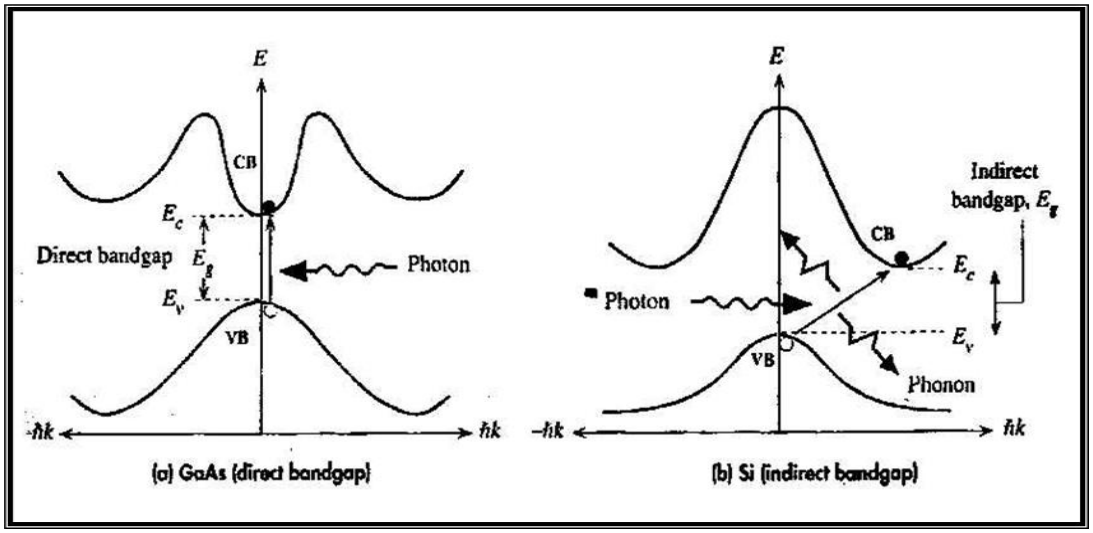

Figure 0.5. Types of gaps in semiconductors with restricted energie (a) Self-direct gap (b) Indirect self-gap [66].

In the following relationship, the equation of the absorption coefficient for the transitions

$$\alpha h\upsilon = B_o(h\upsilon - E_g^{opt.})^r \qquad (3.14)$$

$E_g^{opt.}$: The forbidden gap of optical energy

h : Planck's constant

υ : The frequency of the incident photon

hv: The energy of the incident photon eV

r: a constant whose value depends on the type of transitions; for example, if $r = 1/2$, the transition is direct and allowed, and if $r = 2/3$, it is direct and prohibited.

Either if indirect is permitted $r = 2$ or if indirect is prohibited $r = 3$, keeping in mind that neither type of direct transition is temperature-dependent and only appears in semiconductors with a direct self-gap [63].

3.9. OPTICAL ENERGY GAP

It known as the lowest energy necessary for electrons to move from the top of the valence band to the bottom of the conduction band (EG). The type of practical application that is suitable for the energy range of the photons falling on the thin film in the production of electronic devices such as solar cells, detectors, photodiodes, and solar collector coatings of both types, transmitting and reflective, it is necessary to calculate the value of the optical energy gap (Eg^{opt}) for the prepared film. Temperature, inoculation, and other preparation variables, as well as the preparation process, all have a modest impact on their worth. Pure semiconductors Eg^{opt} is not entirely free because there are regional levels brought on by structural flaws. The data on observed absorbance at wavelengths used to calculate it. Equation 3.13 ($h\nu$) allows us to calculate the optical energy gap Eg^{opt} of films that made by standard procedures as a function of incident energy ray hν. This done by extending the straight portion of the curve until it intersects the energy axis at ($0 = \alpha$), which provides us with a value. Laser energy gap Eg^{opt} [67].

3.10. ELECTRICAL PROPERTIES

One of the most significant qualities that set semiconductors apart from other materials is their electrical properties, which influenced by a variety of preparation circumstances and preparation techniques, the most significant of which is.

First: D.C Electrical Conductivity

The movement of charge carriers through a solid using an electric field produces the electrical conduction current. The observable current in metals brought on by free electrons. In semiconductors, a small number of atomic vibrations are enough to break the connection, releasing the electron to roam freely inside the crystal. Two different types of charge carriers will thus participate in the conduction process, and the electrical conductivity σ of semiconductors determined by the following relationship. It is known as the conduction electron, leaving behind a gap, and it participates in the

conduction process by moving in the opposite direction to the movement of electrons and in the direction of the field itself [68].

$$\sigma = J/E = e\,(n\,\mu_e + p\,\mu_h) \tag{3.15}$$

J: electric current density, E: the intensity of the applied electric field
e: charge of an electron, μ_e: Electron Mobility, μ_h: vacuole motility
n and P: hole concentration and electron concentration, respectively.

The final equation seems to indicate that electrical conductivity is dependent on two fundamental variables: the concentration of charge carriers and their mobility when subjected to an electric field. These two variables change depending on temperature, inoculation ratios, and processing conditions. The electrical resistivity ρ is the inverse of the Electrical Conductivity(σ_{dc}), as shown in the equation below.

$$\sigma_{dc} = \frac{1}{\rho}\,(\Omega.\,cm^{-1}) \tag{3.16}$$

$$\rho = R\,\frac{\text{Å}}{L} \quad where\,\{\,\text{Å} = b\,.\,t\,\} \tag{3.17}$$

σ_{dc}: Continuous electrical conductivity
ρ: Resistivity
R: electrical resistance in Ω
L: Aluminum pole distance cm
Å: The cross-sectional area through the thin films for electrons
b: pole width cm, t: thin film thickness and measured nm and convert unit cm

Second: Activation Energy:

The Arrhenius equation can be used to express how electrical conductivity changes with temperature since semiconductors have a resistance with a negative thermal coefficient and often respond exponentially as a function of temperature [69].

$$\sigma_{dc} = \sigma_o \exp\left(\frac{-E_a}{K_B T}\right) \quad (3.18)$$

k_B: Boltzmann constant $k_B = 1.38 \times 10^{-23} \mathrm{J/K} = 0.086 \times 10^{-3} eV/K$

σ_o: It has a low metallic conductivity, E_a: Activation energy for electrical conductivity eV and corresponds to $E_c - E_f$

T: It represents the absolute temperature It measured in Kelvin degrees k

According to the following equation 3.18, the slope of the line will be equal to - if it is drawn σ_{dc} vs. $1/T$, and then the activation energy will be measured E_a in units eV.

$$E_a = slop \times k_B \quad (3.20)$$

Additionally, it is evident from equations 3.14 and 3.17 that the relationship between the product of carrier concentrations and mobility as a function of temperature change determines how conductivity changes with temperature.

3.11. HALL EFFECT

The change in current distribution in a conductive or semi-conductive chip caused by the action of the magnetic field known as the Hall Effect. As shown in the diagram of Figure 3.6, when a magnetic field, let's say B_Z, is applied in a direction perpendicular to an electric current I_X flowing through a semiconductor in the x-direction, the electrons carrying the current deviate towards the left side, making this side negative about the right side, and a potential difference between them appears. Hall Voltage V_H has been measure. A semiconductor of the negative type experiences this, whereas a semiconductor of the positive kind experiences the opposite. This discussed as to why it occurs. The Lorentz force, which identified by using the right-hand rule emerges as a result of this deviation and is perpendicular to both the direction of the current and the magnetic field. By continuing to accumulate negative or positive charges on one side, an equilibrium eventually reached at which the current completely disappears because a force opposite to the Lorenz force due to the emergence of an electric field is present. Credit for identifying this phenomenon originally belongs to the researcher

(Hall) in (1879). The most crucial use of G for semiconductors is to assess the quality of the semiconductor, whether it is positive or negative, and to calculate the values of electrical characteristics like mobility, carrier concentration, and conductivity. The following equation was created using physical relations follows[70].

$$E_H = -\left(\frac{1}{ne}\right) J_x B_z \tag{3.21}$$

It demonstrates that the (Hall) field in the semiconductor is of the negative type, proportional to the density and intensity of the magnetic field, and the Hall coefficient, which written as follows when using the calculation's dimensions, is the constant of proportionality.

$$R_{+1} = -\left(\frac{1}{ne}\right) = \left(\frac{V_H \cdot t}{Ix \cdot B_Z}\right) \tag{3.22}$$

B_Z: projected magnetic field, t: the thickness of the semiconductor slice

Despite its apparent simplicity, this connection is crucial for understanding electrical conductivity σ in solid materials. The density and type of charge contributing to conduction established by understanding each value's signed (R_H), which is negative for semiconductors of the type n-type and positive for the type P-type. The following relationship yields the value of the dominant charge's motion [70].

$$\mu_H = |R_H|\sigma \tag{3.23}$$

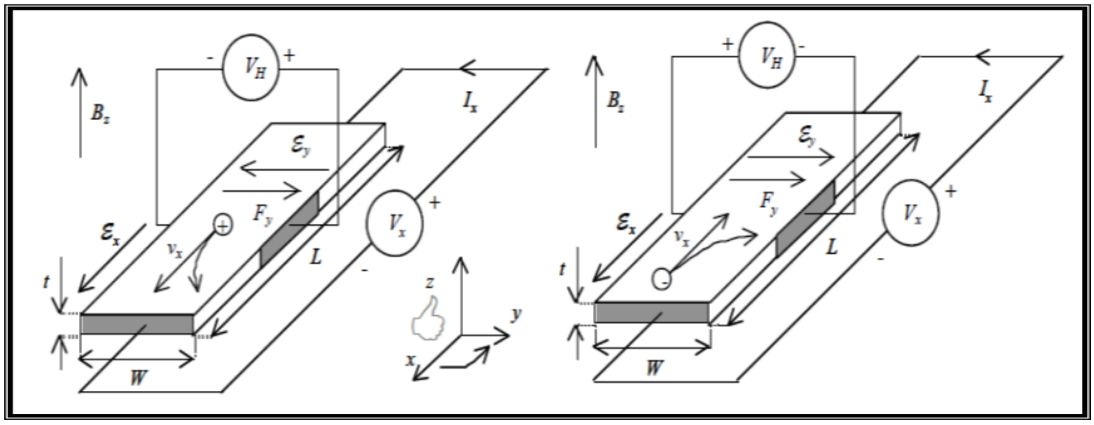

Figure 0.6. Hall effect in semiconductors (a) p-type (b) n-type [71].

3.11. CURRENT-VOLTAGE CHARACTERISTICS

Stuckian's behavior shows its characteristics, through which we will see the behavior of Stuck and that the theory of thermal emission controls the current mechanism, which we will see through.

$$I = I_{s_0}(e^{\frac{-qV}{\beta k_B T}} - 1) \tag{3.24}$$

I_{SO}: reverse saturated current

$$I_{s_0} = A_{sh}A^*T^2\, e^{\frac{-q\varphi_B}{k_B T}} \tag{3.25}$$

*A: Richardson's effective constant, A_{sh}: Schottky contact area, q: charge of an electron

T: absolute temperature, k_B: Boltzmann constant, φ_B: An ideal factor is the barrier height

$$\beta = \frac{q}{k_B T}\left[\frac{V_F}{\ln\frac{I_F}{I_{S_0}}}\right] \tag{3.26}$$

V_F: forward bias voltage, I_{S0} and I_F: forward bias current

Equations used to obtain the values of the saturation current, Schottky barrier height, and ideality factor from the I-V characteristics data 3.23 and 3.24 the slope of (I) against the plot of (V) in the voltage range from zero to value was used to obtain the ideality factor value, moreover, the relation used to compute the tunneling constant.

$$A_t = \left[\frac{d \ln \frac{I_{F_2}}{I_{S_2}}}{dV} \right] \tag{3.27}$$

I_{S2}: saturated stream, I_{F2}: It is located in the tunnel area, which is a forward stream.

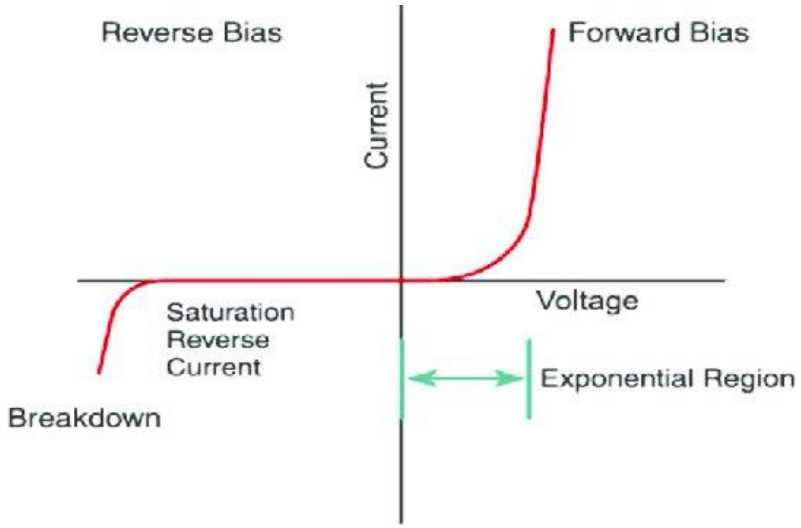

Figure 0.7. Schtucky's current-voltage silicon junction behavior [72].

3.12. TIN OXIDE

The tin oxide material is in nature in the form of salts, its color is transparent and sometimes it is gray. Its external structure is not uniform in shape, and through its structure examination with a microscope. Its corners are quadruple and has a low resistance ranged (3- 10 Ω. cm). One atom of oxygen surrounded by four atoms of tin, it called a semiconductor because it is a mixture between insulators and conductors. Every semiconductor material has several energy gaps, and this thing applies to tin, as it ranges from 3.6 eV to 4.6 eV, where in the following table show some of the properties of thin films [73] [74].

Almost all chemicals oxidized and have resistance to heat and pressure. As for tin oxide, it is stable at room temperature and can withstand high temperatures. The origin of metal belongs to the (TCO) family, meaning it can resist low-voltage electricity and combines optical properties at the voltage level. which we can see with the normal eye [73].

Thin films used in the field of micro-electrochemical devices. In our study, we will discuss tin oxide, which is a direct entry into solar cells, as well as its many uses such as smart glass, mobile phones, gas sensors, coatings, and electro-optical pulses [75].

Table 3.1. In this table we will see some of the properties of tin oxide from the physical and chemical points of view.

Lattice constants	**(a=b= 4.737، c= 3.826) (Å)**
Density	6.95 (gm / cm^3)
Refractive index	2.0
Band gap	3.67 (eV)
Color	White
Melting point	1630°C
Boiling point	1800-1900°C
Appearance	White powder
Solubility in water	Insoluble
Crystal structure	Rutile(tetragonal)
Coordination geometry	Octahedral (Sn^{IV}); trigonal planer (O^{-2})
Molecular weight	150.69 (gm/mole)
Type conductivity	n-type

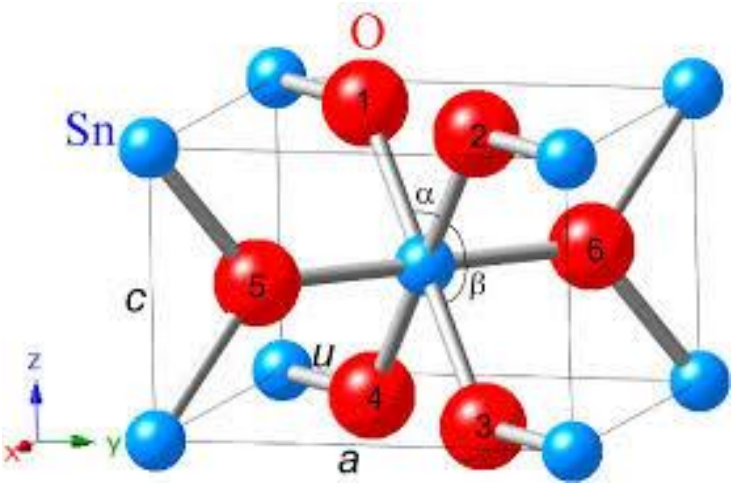

Figure 0.8. Under the microscope, we will see the bonding of the oxygen atom with tin atoms [76].

The presence of oxygen with a compound SnO_2 makes it non-stoichiometric, as the formula of a compound SnO_2 makes it SnO_2-x, where the x represents a stoichiometric quantity, where in the previous figure, the previous words are shown, and they have known constants ($c = 3.188\,Å$) ($a = b = 4.737\,Å$)[77].

PART 4

MATERIALS AND METHODS

4.1. INTRODUCTION

This chapter discusses deposition techniques and some of their benefits, the components of a thermal evaporation device, process of making samples, how to clean glass slides and the method of deposition. It also demonstrates how to measure thin film thickness and the instruments used to measure structural and optical properties.

- Clean the glass on which the substance deposited.
- Grinding, preparing, pressing, and mixing the material
- Precipitation Sn pure
- Oxidize the films for two hours in the oven at 450 ℃
- Measurements

4.2. THERMAL EVAPORATION UNDER VACUUM METHOD

This method considered one of the best methods for preparing thin films because this method has a set of advantages that differ from other methods and these advantages as posterior.

- Obtaining thin films of high purity by vaporizing the Sn material in a vacuum chamber to remove most gases and other vapors, preventing the thermal oxidation process of the thin film from happening in the presence of oxygen gas, and removing dust and other particles that could cause defects in the prepared thin film's crystalline structure.
- As the melting point of the substance decreases with a decrease in pressure, the degree of high vacuum and low-pressure 10^{6}- 10^{-9} mbar inside the

evaporation chamber prevents the occurrence of pollution. It also lessens the likelihood of collisions (scattering) between the atoms of the vaporized substance and the atoms of other gases within the evaporation zone.

- Obtaining a thin film with a low center of effort, and this thing results from the presence of a small number of foreign atoms.
- In addition to making sample preparation simple, this method protects the floors (bases) that have been set up for sedimentation from surface damage while also allowing for the quick collection of numerous samples with identical preparation conditions and thickness.
- The thermal evaporation method in a vacuum has several drawbacks in addition to its benefits, such as the following: It is not appropriate for making thin films for compounds (compound semiconductors) since the slow increase in temperature works to separate the components of these compounds. It is a restricted technique for evaporating substances and elements at high temperatures. Low melting, some of the evaporated material is lost inside the evaporation chamber. The created film adheres to the substrate to a lesser extent than with atomization, and it is impossible to prepare a large-area film.
- The air pressure inside the evaporation chamber, the temperature of the base that is ready to be sediment. The degree of cleanliness of the chamber and floors from contamination, the rate of sedimentation, the distance between the basin and floors, the type of material and the appropriate shape of the basin used to evaporate the mixture are the most significant factors that affect the process of creating thin films using the thermal evaporation technique in a vacuum. These variables are crucial in influencing the homogeneity, cleanliness, and exposure of the produced film to oxidation as result of the collision of the material's vapor atoms with the air atoms inside the vacuum chamber.

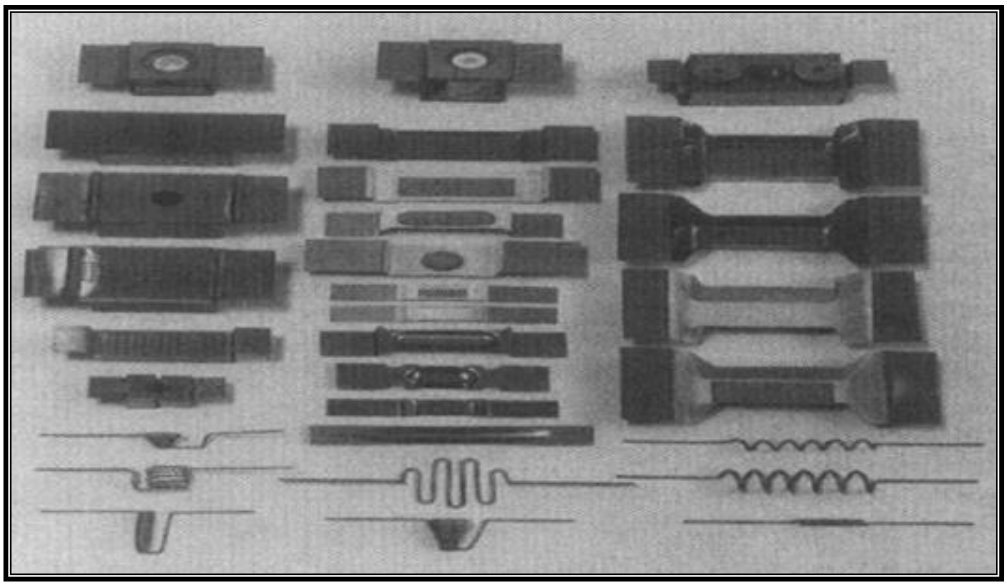

Figure 0.1. Set of vesicles used in this process.

After the degassing procedure, there are three steps in the deposition process for the film prepared in this way: The first step is to heat the tank to the point where the material evaporates and then change the material to be deposit from solid to gaseous state after depositing it in the tank. The atoms then move from the evaporation (heating) source to the floors, where they condense and settle to form deposits on the floors, ready to be deposit. Since the evaporation basin and the sedimentation, floors are connected and on opposite sides of the chamber, it is necessary to know the appropriate air pressure (mbar or Torr) inside the chamber to obtain the necessary conditions for evaporation in the vacuum. This means that the amount of the free path rate must be greater than the distance between the evaporation basin and the sedimentation floors and the minimum amount $P = 10^{-4}$ Torr for the discharge pressure.

4.3. VACUUM THERMAL EVAPORATION SYSTEM

1- Evaporation Chamber

The bell jar, which is a metal cylinder that resists rust and corrosion and has a high capacity to withstand high temperatures and low pressure for sedimentation, as well as the evaporation basin, which comes in a variety of shapes and types, are some of the

basic components included. Materials for manufacture shown in figures 4.2 according to the composition and shape of the evaporating substance. The heating poles that the basin built with and the basin itself are frequently composed of high-melting materials like molybdenum M_o or tungsten W. It tightly controls the amount of voltage needed to evaporate the material. It is also equipped with the right voltage. The substrate holder, which is where the samples installed, expands by using an electrical transformer outside the evaporation chamber. It also regulates the vertical distance between the basin and the samples. It also has an electric heater that heats the floors to the temperatures that a thermocouple measures.

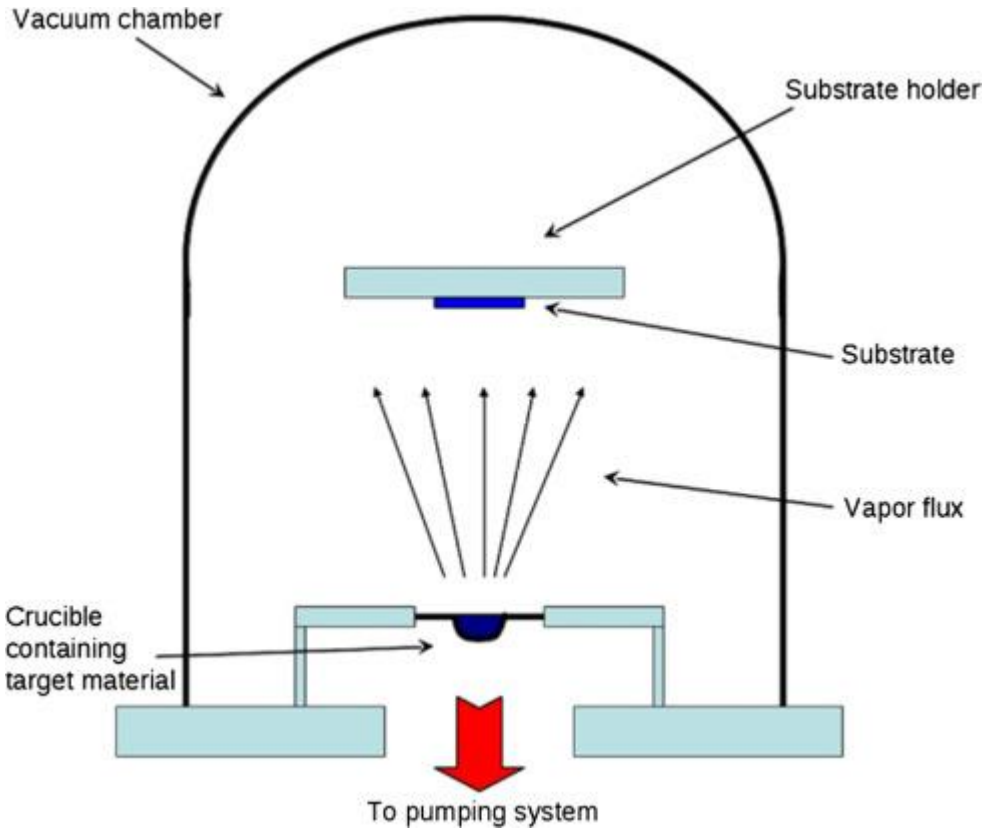

Figure 0.2. Illustration of the thermal evaporation chamber [78].

2- Vacuum Pumps

Because they form the backbone of the process of reducing pressure to low pressures adequate to finish the sedimentation process, pumps are among the crucial components of the thermal evaporation system in a vacuum. By using numerous linked pumps that operate in tandem and chilled by liquid nitrogen or cold water, low pressures of less

than 10^{-10} Torr can be achieve. Two major pumps that worked together used in this study's thermal evaporation system in Hoover.

Rotary Pump - B- Diffusion Pump

The return and leakage of evaporated oil particles into the evaporation chamber during the evaporation process, which has a detrimental impact on the created thin film's purity, is one of the key issues the diffusion pump must deal with in its daily operations. Thin films and these issues can be resolved by cooling with liquid nitrogen or cooled water.

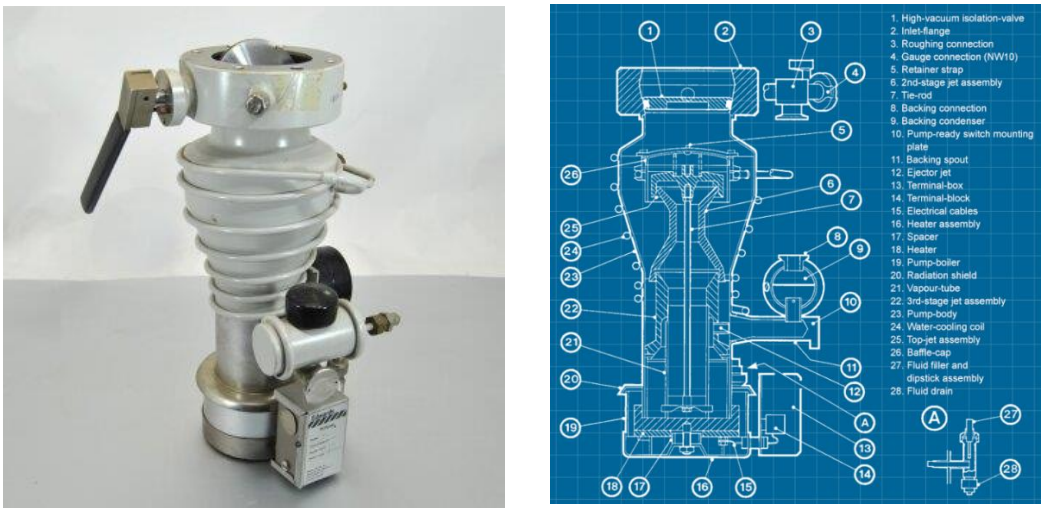

Figure 0.3. Depict a detailed inside view of the Diffstak 63 diffusion pump used in sedimentation.

3- Vacuum Gauges

Two scales used in the system.

It works with a range $1 - 10^{-3}$ Torr as shown in figure 4.3, and when the first pump turned on, it will be suitable for measuring the pressure inside the chamber.

4- Pirani gauge

It works with a range 10^{-2}- 10^{-7} and when the second pump turned on, it will be suitable for measuring the pressure inside the chamber.

5- Cooling System

Depending on the kind and effectiveness of the liquid used in the cooling process during the operation of the evaporation, either liquid nitrogen gas or cooled water, the thermal evaporation system's cooling system plays a significant role in obtaining the required degrees of air pressure in a short amount of time, which is used to cool the aforementioned system.

(a) (b)

Figure 0.4. Shows the very low pressures in the digital PINK scale.

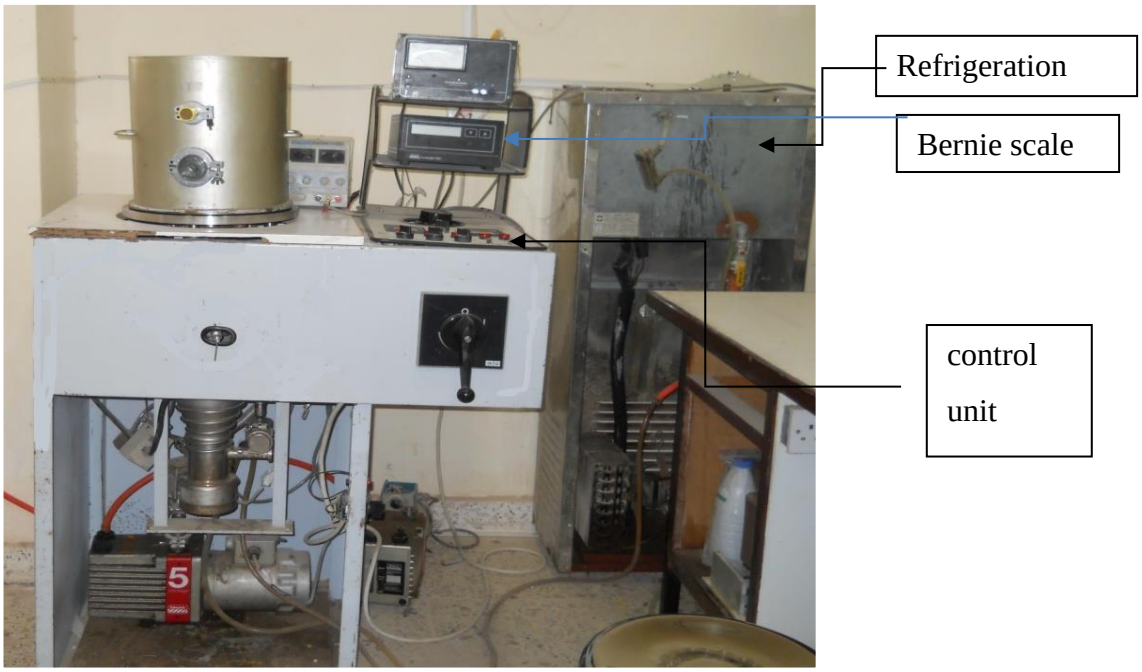

Figure 0.5. The thin film preparation system.

4.4. CLEANING OPERATIONS

4.4.1. Clean the Device

The device was broken down into small pieces for this procedure, the pieces were then cleaned using a solution made by mixing ethanol and distilled water in a 3:1 ratio, placed in a spray bottle, dried by a hot air pump, and then grease (ointment) was applied to the parts. After operating the device, the pressure dropped to the lowest level possible 5×10^{-5}- 3.0×10^{-5} mPa to check for any flaws, and the device's joints cleaned with sandpaper to prevent dust or air from leaking into the interior during operation. After that, clean with the combination.

4.4.2. Clean the Boat

The molybdenum M_o basin cleansed in simple water, thoroughly rinsed, and then submerged for an entire hour in distilled water, pure acetone, and alcohol. It then heated to the point of incandescence for some time to evaporate any traces of the suspension material, which used to make both previous two materials and allows the basin to be bend and wasted easily but, when heated, turns into glass and breaks easily,

so it must be handle carefully, as shown in the figure 4.6. The basin dried using a hot air pump.

Figure 0.6. The template used in the deposition process.

4.4.3. Substrates Cleaning

There are two types of flooring for thin film deposition.

- The first kind: Bases made of glass, thickness is 1 mm and dimensions are $26 \times 76mm^2$, and the process of cleaning the glass goes through stages, including.
- We bring plain water and mix it with several cleaning powders to remove stains, dust, and dirt on its surface, and then we put it under the water tap for 15 minutes.
- In distilled water, we put the slides and put it on the vibrator, and it will wash the bases. The principle of the device is ultrasonic waves for a period of 5 minutes.
- We put the bases after that with ethanol alcohol C2H2OH and wash them with an electric vibrator for a period of 15 minutes, and the alcohol is pure 99.
- We use filter papers to dry the bases, using a blower device with hot air, and then the bases placed in a stabilizer and inserted into the fumigation system.
- The second kind: It shall be a single crystal, which are bases of silicon, and its type shall be p-type, and electrical resistance shall be $1\Omega.\,\mathrm{cm}$, and its crystal orientation shall be 111, and its thickness shall be $200 \pm 30\mu\mathrm{m}$ and shall be of German origin and from deutsche solar AG and the stage of cleaning is.
- Cut to dimensions of $(25 \times 20 \times 0.2mm^3)$.

- They properly cleaned by submerging them in the same basin of the prior ultrasonic oscillator for the same amount of time first with distilled water, then with ethanol 15 min.

4.5. FORM PREPARATION PROCESS

Figure 4.7d shows an agate mill used to grind Tin Sn into powder. Figure 4.7a shows a four-level sensitive balance used to measure the melting point of tin Sn, which has a purity of 99.9 % and made in India. The amount of the material is 0.012 grams, which ground in a mill and a pressure mold, then mixed with an agate grinder for half an hour. It then placed in the mold to compress the material into a 10 mm disk, figure 4.7b, and the sample is then compressed. Samples extracted using a five-tone hydraulic press for five minutes and heated to 100 ℃ in an oven for one hour. After they removed, cooled and placed in a plastic container as shown in figure 4.7c. Pressure used to bring the material closer to its evaporation temperature to prevent it from separating during deposition.

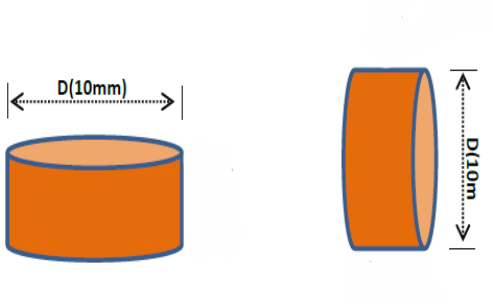

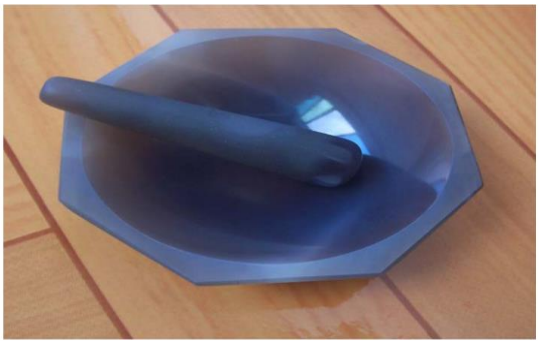

Figure 0.7. a) Sensitive Libra, b) User template, c) compressed sample form, d) The agate grinder.

4.6. PREPARATION OF THIN FILM

- The samples are prepared in this manner and placed in Tikrit University's vacuum evaporation system by weighing a small portion of the compressed sample in a sensitive balance, as shown in Figure 4.7 a, at a weight of $0.0045 - 0.0040$ gm in the same weight. As shown in figure 4.6, position the pure material model to the same thickness as feasible in a molybdenum Mo basin that is 3 mm deep.
- The gadget then turned on once the bases secured to the floor stand. After several tries, a thin, uniform thin film with good adhesion w achieved at a height of (10 cm), and the ideal spacing found between them.
- The mechanical pump system turned on until all air removed, at which point it moved between the first and second chambers until the pressure jumps to 10-3. The diffusion pump's oil heater then turned on, and after a while, we hear the oil crackling, which opens the sedimentation chamber valve. The diffusion pump and sedimentation occur at an average pace to prevent separation of the mixture after a period of time we attain the appropriate pressure between 5×10^{-5}- 3×10^{-5} mpa.
- Following sedimentation, samples removed from the apparatus and put in an oven for two hours at $450°C$ to undergo thermal oxidation. The use oven shown in Figure 4.8.

Figure 0.8. Annealing furnace.

4.7. OHMIC CONTACTS AND ELECTRICAL DEPOSITION

It is important to execute the ohmic contact process between the electrical wires and the surface of the semiconductor material to examine the electrical characteristics of the manufactured thin films as well as the optical and gas sensitivity characteristics metal contact with a semiconductor and no resistance added to the resistance of the semiconductor. By employing the same thermal evaporation method from before and applying low pressure of $(5 \times 10^{-5}$ mPa) , a coating of pure aluminum 99.99 % with a thickness of (200 nm). Aluminum rods that will serve as connecting electrodes are first weighed using a sensitive scale before inserted in a tungsten basin for electrode deposition figure 4.7. To investigate the continuous conductivity qualities and the effects of the Hall Effect, respectively, on the surface of the sample, aluminum deposited in the shape of a clamp to serve as the electrode linking the gas detectors. Aluminum electrodes are deposited on the silicon floor's lower side and top of the thin film, giving the produced photodetector the shape indicated in the detector schematic in Figure 4.9 a. The generated thin films and reagents can then be attaches to the wires of the external electrical circuit using the silver paste seen in figure 4.9 b to undertake the necessary electrical and photoelectric tests after the electrodes have been place.

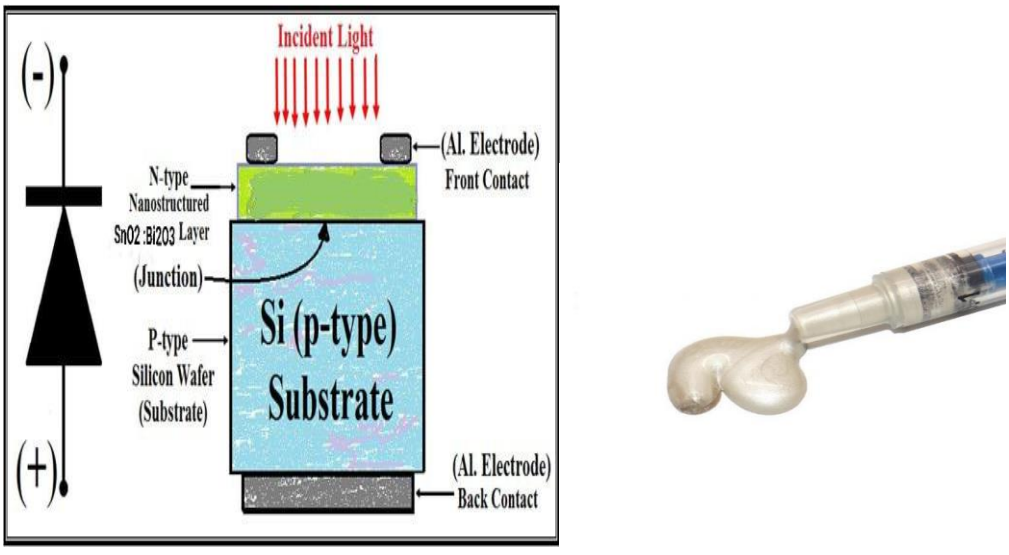

A B

Figure 0.9. Scheme to show how photovoltaic detectors are manufactured.

4.8. OPTICAL MEASUREMENT

As the values of the absorbance and transmittance of the prepared films measured as functions of wavelength variation, the optical measurements also included a spectroscopic measurement of the transmittance T and absorbance A of the prepared films using a device UV-Visible 1800 Shimadzu Photometer, as shown in Figure 4.10. The device turned on within the range of nm 300-1200, the slides are removed until it is fully functional, the device is reset by pressing the (AUTO ZERO) button, and then a glass slide is introduced to measure its transmittance as a reference slide. Next, another slide of the same type is introduced, on which the thin film is deposited, and by deducting the transmittance values of the unlabeled slide from the transmittance values of the other slide, the device.

Figure 0.10. UV device.

4.9. INVESTIGATION OF THE STRUCTURAL OF PREPARED FILMS BY XRD TECHNIQUE

An X-ray diffraction equipment of the type - SHIMADZU-Japan-XRD 6000 used to diagnose the nature of the crystalline structure of the pure thin SnO_2 films and to examine the effect on the composition of these manufactured films. This method can determine the structure of solid materials, whether they are monocrystalline, polycrystalline, or amorphous, and it provides data in a specific table that accurately displays the diffraction angle 2θ, the distance between crystal planes d_{hkl}, Miller coefficients h, k, l, the intensity of each peak, and the width of the curve at the peak's maximum intensity (FWHM). Knowing that the X-ray diffraction device XRD used in this study complies with the following specifications, the type and nature of the crystalline structure of the prepared film material are determined by comparing the values of the obtained XRD results with the values of the standard (ASTM) results table for the film material SnO_2.

X-Ray Tube	Scanning Measurements
Target: Cu kα.	Axis: Theta – (2θ).
Wave Length: (λ of X-Ray) =1.5406 Å.	Scan Mode: Continuous Scan.
Voltage: 40 k Volts.	Range: 25-75 deg.
Current: 30 mA.	Step: 0.05 deg.
	Speed: 5 deg./min.

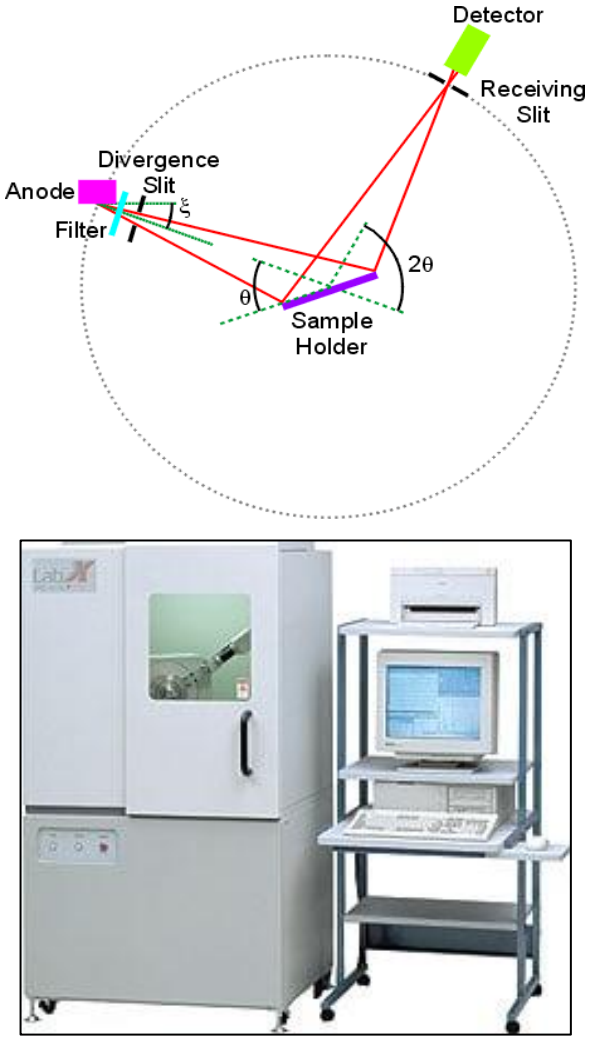

Figure 0.11. X-ray machine.

4.10. HALL EFFECT MEASUREMENT

To determine the type of primary charge carriers by determining the Hall coefficient RH, via which the concentration of carriers n and their mobility μ are determined, the Hall effect at room temperature was evaluated on all prepared films deposited on glass floors, utilizing the electrical circuit depicted in figure 4.12 a. The constructed thin film was positioned perpendicularly in front of a preset magnetic field B_Z and its strength equals B = 0.5 tesla perpendicular to an electric field passing through the sample, as two electrodes were connected, after conducting electrodes were deposited on it figure 4.12 b. To measure the current flowing through the thin film I_x, two parallel thin film electrodes were connected by insulated copper connecting wires to a continuous power supply (D.C. Power Supply) type (Dazheng: PS-303D), while the

two poles were linked in parallel. To measure the Hall voltage V_H produced on both ends of the thin film, the other two thin film parallel electrodes connected in parallel by insulated copper connecting wires. It should be mentione that the two digital ammeters and voltmeters are of the type UT136 and supplied by the Japanese firm and that the process of joining the copper wires with the electrodes of the thin film accomplished by employing silver paste welding paste. The thin film's current I_x measured by the ammeter using a voltmeter, note the Hall voltage V_H produced at the thin film's two ends.

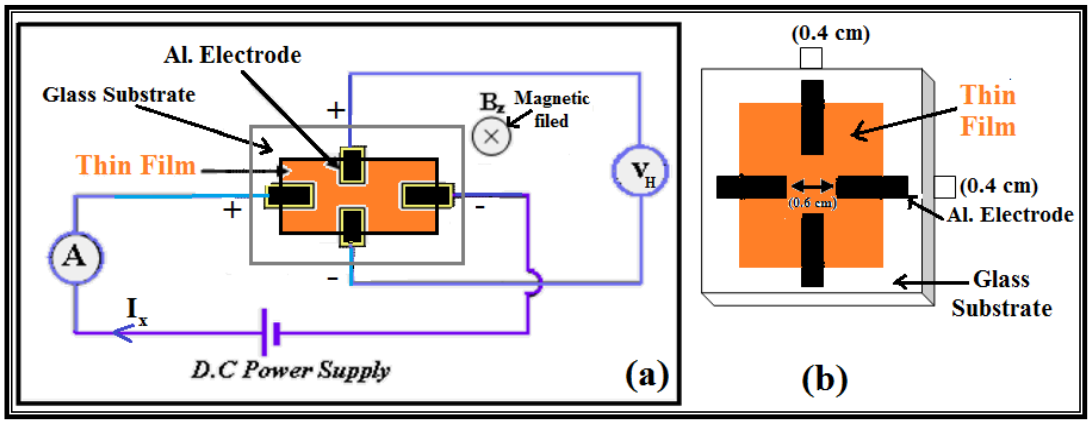

Figure 0.12. The circuit used to measure the Hall effect b-Schematic depicting the sample's shape following the application of conduction electrodes to evaluate the Hall effect.

4.11. RADIOACTIVE SOURCES

The thin film irradiated with gamma by radioactive source ^{60}Co for one- and two-weeks using gamma chamber 900, this system valid in science faculty / Baghdad University. This source ^{60}Co emits mono-energetic 1.173 and 1.332 MeV and has a half-life of 5.3 years.

Special shielding needed for gamma ray sources with high activity more than a few curies, and many Innovative forms have been create. Figure 4.13 illustrates how the source has been integrate into a lead container with facilities for inserting chemicals without subjecting the operator to radiation.

Figure 0.13. Gamma radiation device.

That the radiation spreads in all directions and gives us a dose of 13 rad per hour.

The neutron source ^{241}Am - ^{9}Be with activity of (3.5×105 neutron/ cm2. sec). use to emit fast neutron with energy of 5 MeV, this system valid in college of Education for pure science Ibn- Al Haithem / Baghdad University. The thermal neutron gets out by using paraffin wax shield surrounding the radioactive source as shown in figures 0.14 and 4.15. For protection, the shield surrounding the source is made of paraffin wax, and there are other shields such as sand and water. The tin oxide films irradiated for 1 and 2 weeks. The doses calculated shown in table 4.1.

Table 4.1. Radiation dose results in rad.

Time	**For γ**	**For n_{th}**	**For n_{fast}**
7 days	314.244	304575.539×10^5	304575.539×10^5
14 days	628.489	609151.079×10^5	609151.079×10^5

In the following picture, we will see the neutron irradiation chamber, and as we see the barrier is paraffin wax.

Figure 0.15. Profine wax neutron shield.

Figure 0.16. Example of thin film near irradiation.

PART 5

RESULTS AND DISCUSSION

First, the energy gap. The optical energy gap for the permissible direct transitions can be calculate by drawing the linear relationship in the values of a, b, and c with the photon energy, as shown in figures 5.1 a, b, c and d for non-irradiated films and films irradiated with gamma and thermal and fast neutrons, respectively.

It found that there is a slight change in the energy gap, as shown in Table 1 and Figure a, which shows a decrease in the energy gap with the process of irradiation with gamma rays, thermal and fast neutrons. This is due to the possibility of changing the phase of the material after irradiation, and this is consistent with the results obtained by reference [32].

The optical properties included the following. Secondly, the transmittance spectrum. Transmittance measurements carried out in the wavelength range 190 to 11.00 nm for all non-irradiated films, irradiated ones, and those irradiated with gamma rays of energy 1.173 and 1.332 MeV emitted from a ^{60}Co source for a period of 7 and 14 days with a radiation dose. 314.242 rad and 628. 489 as well as irradiated with thermal and fast neutrons issued from a source ^{9}Be – ^{241}Am for a period of 7 and 14 days with radiation doses 6.092×10^{10} , 3.046×10^{10} on a centimeter. Tin oxide, S_nO_2, considered one of the semiconductor materials with high transmittance atoms in the visible and permeable region, as the figures showed a, b, c are few in the ultraviolet region with a gradual, quasi-stable increase starting from a wavelength 191 nm. This behavior is identical to the behavior of the transmittance curve in a group of transparent conductive glasses, where the transmittance increases rapidly at the cutting-edge point, which confirms the energy gap in thin films is of the direct type. The transmittance spectrum depends on the chemical composition of the material, the thickness of the membrane, the topography of the surface, and its reflectivity. The figures also show a

high transmittance of 96 % for the visible and infrared regions, which can be used to manufacture a photodetector. Figure 5.2 a, for the fully irradiated films shows the same dispersion for the irradiated and non-irradiated films for a period of 7-14 days. The effect of radiation presented by an increase in the transmittance to more than 93 % in the ultraviolet UV region for wavelengths ($193 - 420$ nm), and the irradiated transmittance of the film for 14 days was slightly greater than seven days. As for Figure 5.2 b, we find that the transmittance spectrum is the same for non-irradiated and irradiated thin films, but an increase in transmittance to more than 93 % observed in the UV region for wavelengths ($193 - 430nm$), but the transmittance of the thin film irradiated for 7 days is greater than the rest. As for Figure 5.2 c, the thin film showed non-radioactive and radioactive behave in the same way. There is a complete match between them, which indicates that the thin film not affected by fast neutrons. Because the cross-section of absorption is small, $\sigma a \approx 0.01$ barn, compared to the cross-section of the thermal neutron reaction, which is $\sigma a \approx 0.626$ barn. This agrees with the reference [30].

Thirdly, absorption. Absorption generally depends on the energy of photons falling on thin films and semiconducting materials. The absorption edge represents the dividing line between the point of high light absorption and the transparent region. Through the figures 5.3 a, b, and c, the absorption spectrum of the films, which are non-radioactive and those irradiated with gamma rays, thermal neutrons, and the fast neutrons as a function of wavelength, respectively. The figures showed the same behavior for all irradiated and non-irradiated films for the spectral range 586- 1100 nm, the absorbance was less than 0.016, which can be consider the edge of absorption, because the absorbance increases after that in the spectral range 193- 585 nm. Where we find the simple shift of absorbance to be the irradiation period of seven days has less effect than day 14, which in turn less absorbent without irradiation.

The absorption coefficient calculated for non-irradiated films, irradiated films with gamma, thermal, and fast neutrons, based on the absorption spectrum as a function of wavelength. Figures (5.4 a, b, and c) showed that the change in the absorption coefficient with the energy of the incident photon hυ, which remains that the behavior of the absorption coefficient is not Similar to the absorbance. We find that the curve

of the non-irradiated thin film at the wavelength increases, reaching its peak at the wavelength 315 nm, after which it begins to decrease up to 294 nm and fluctuates up to the wavelength of 195. As for the thin film irradiated with gamma rays, we find that irradiation for 7 days reduces the absorbance. For most of the wavelengths, it increases slightly at wavelengths less than (300 nm). As for the films irradiated for 14 days, they showed the same behavior as the non-radioactive films, but with an increase in absorbance starting at 470 nm and reaching the peak at (232 nm), with a high absorbance of only 0.3645 estimated to be twice the absorbance of the non-irradiated thin film. The absorption coefficient of the materials irradiated with thermal neutrons increased the absorbance of the irradiated thin films compared to the non-irradiated thin films but. They had the same behavior at some wavelength ranges from $456 - 1015$ nm the peaks are at a wavelength of 210 nm, and it appears that the absorbance has increased for the irradiated thin film for seven days more than 14 days. When they irradiated with fast neutrons it also appears that the absorbance has increased for the thin films irradiated with fast neutrons compared to those that non-irradiated. There is shift in the peaks that represent the highest absorption of the thin film. It was 0.1628 au at the wavelength of 248 nm for the irradiating film for 7 days, 0.1419 au at 220 nm for the irradiating film for 14 days, and 0.1186 auat the wavelength of 197 nm from the non-irradiated film. As for reflectivity, it has the same behavior of absorption.

As for reflectivity, it has the same properties as absorption figures 5.5, 5.6 and 5.7.

As we can see in figure 5.8 a show the current-voltage characteristics of the non-radiated SnO_2 thin film, where the relationship between current and voltage can be considered almost an ohmic relationship, as the current is directly proportional to the voltage. This means that the density of the effective carriers N_c in the conduction band much less than the density of the free carriers ($N_\circ$). That is $N_\circ > N$ as in figure 5.8 b of the current-voltage properties for a period of seven days consists of two regions, the first in which the current response is very small with an increase in applied voltages, and the second in which the current response with voltages is very large and clearly a breakdown region at 736 volts. Likewise, figure 5.8 c is for the radiating thin film. 14 days consist of two regions. The first begins at its voltage 410 volts, while the

breakdown region begins at a voltage of 613 volts, figure5.8 d of the thin film irradiated with thermal neutrons for a period of seven days. We find that the first region is very small at its voltage of 988 volts, and the collapse region is at 1002 volts figure5.8 E for the thin film irradiated with thermal neutrons for 14 days, we find that the first region is not small, starting at 894 volts and the breakdown voltage is at 972 volts. Figure5.8 f for the thin film irradiated with fast neutrons, we find that there is only a breakdown region that begins at 781 volts figure5.8 g of the thin film irradiated with fast neutrons for 14 days. We find that there are two regions, the first at 800 volts and the breakdown voltage at (841 volts). Accordingly, we notice that the value of the breakdown voltage of the thin film changes, accompanying a different exposure depending on the type of radiation. This can be explain by the fact that the inner layer of the current carriers, the generation of free radicals increases as a result, of irradiation, which leads to a decrease in the comparison. When irradiation continues, the current carriers will write more energy than they should until they reach a certain value that reduces the generated charge, and this followed by an increase in the breakdown voltage.

The structural properties showed by the XRD results of the non-irradiated film growth of four crystalline directions, of which 101 were prevalent figure a. This corresponds to the global (ASTM) examination card. When the irradiation increases gamma or neutrons, the peaks have disappeared because of the transformation of a matter from poly crystalline to non-crystalline figure (5.9 b, c, d, e, f, and g).

Table 5.1. Hall effect result

Sample	**EG (eV)**
E.g.for pure	3.307(eV)
E.g.for gama7d	3.267(eV)
E.g.for gama14d	3.225(eV)
E.g.for neutron7d	3.306(eV)
E.g.for neutron14d	3.263(eV)
E.g.for fn 7 d	3.233(eV)
E.g.for fn 14d	3.246(eV)

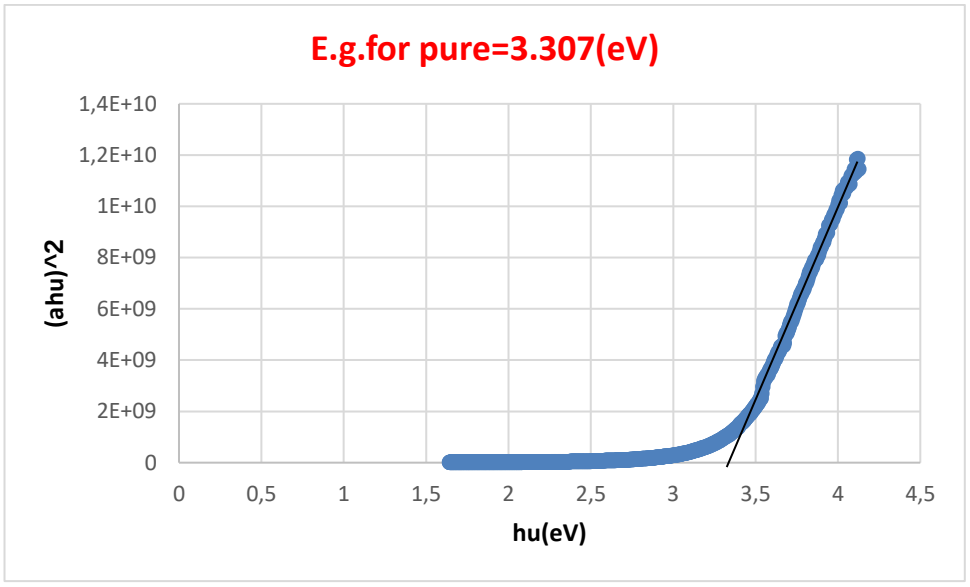
E.g.for pure=3.307(eV)
1,4E+10
1,2E+10
1E+10
8E+09
6E+09
4E+09
2E+09
0
(ahu)^2
0
0,5
1
1,5
2
2,5
3
3,5
4
4,5
hu(eV)

a)

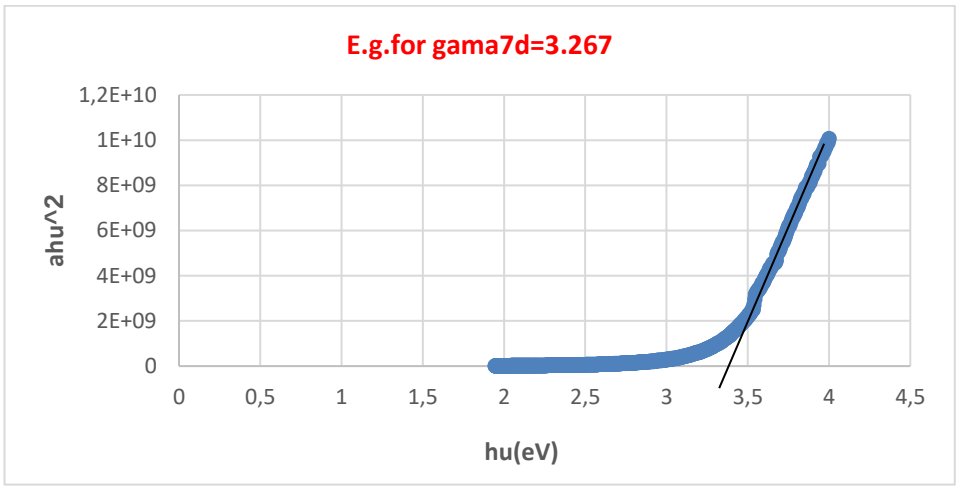
E.g.for gama7d=3.267
1,2E+10
1E+10
8E+09
6E+09
4E+09
2E+09
0
ahu^2
0
0,5
1
1,5
2
2,5
3
3,5
4
4,5
hu(eV)

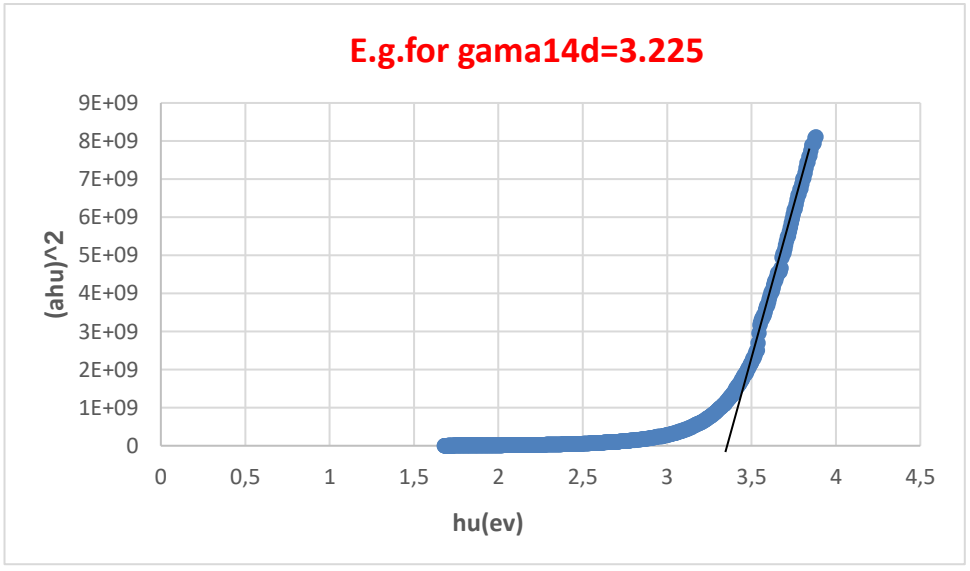
E.g.for gama14d=3.225
9E+09
8E+09
7E+09
6E+09
5E+09
4E+09
3E+09
2E+09
1E+09
0
(ahu)^2
0
0,5
1
1,5
2
2,5
3
3,5
4
4,5
hu(ev)

b)

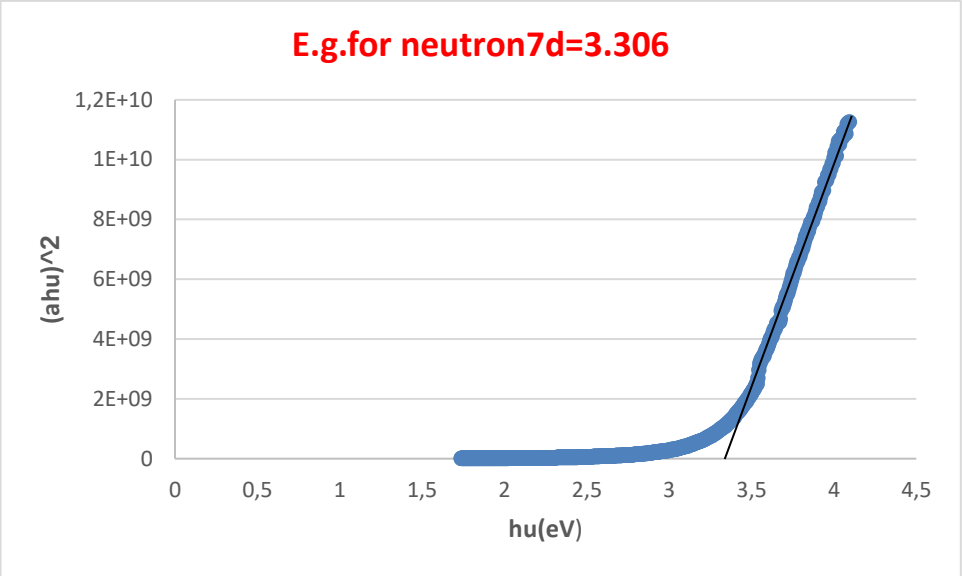
E.g.for neutron7d=3.306
1,2E+10
1E+10
8E+09
6E+09
4E+09
2E+09
0
(ahu)^2
0
0,5
1
1,5
2
2,5
3
3,5
4
4,5
hu(eV)

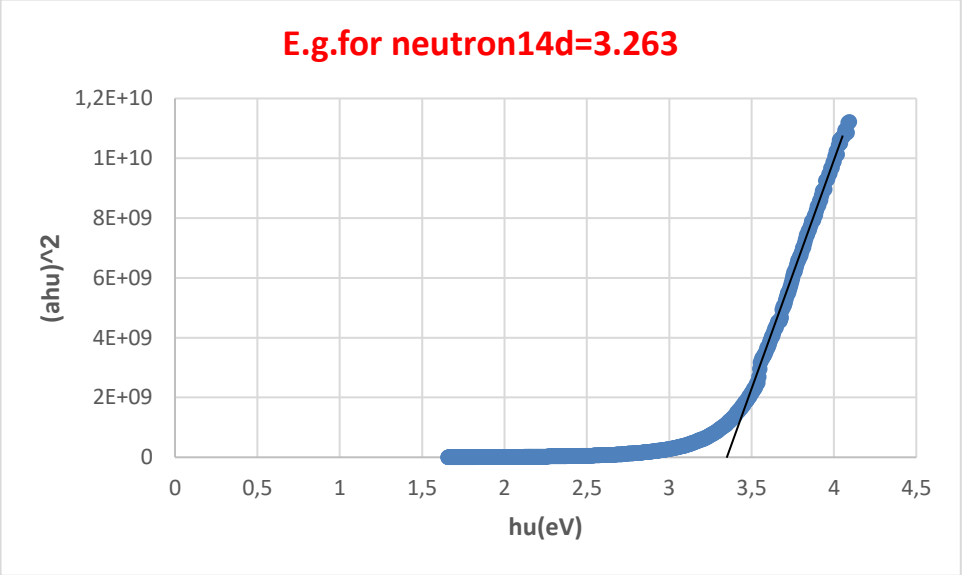
E.g.for neutron14d=3.263
1,2E+10
1E+10
8E+09
6E+09
4E+09
2E+09
0
(ahu)^2
0
0,5
1
1,5
2
2,5
3
3,5
4
4,5
hu(eV)

c)

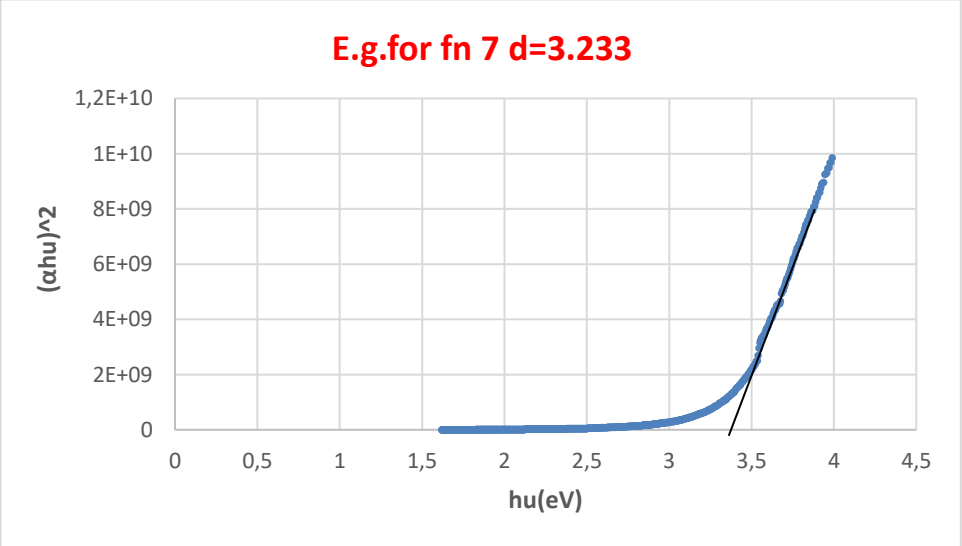
E.g.for fn 7 d=3.233
1,2E+10
1E+10
8E+09
6E+09
4E+09
2E+09
0
(αhu)^2
0
0,5
1
1,5
2
2,5
3
3,5
4
4,5
hu(eV)

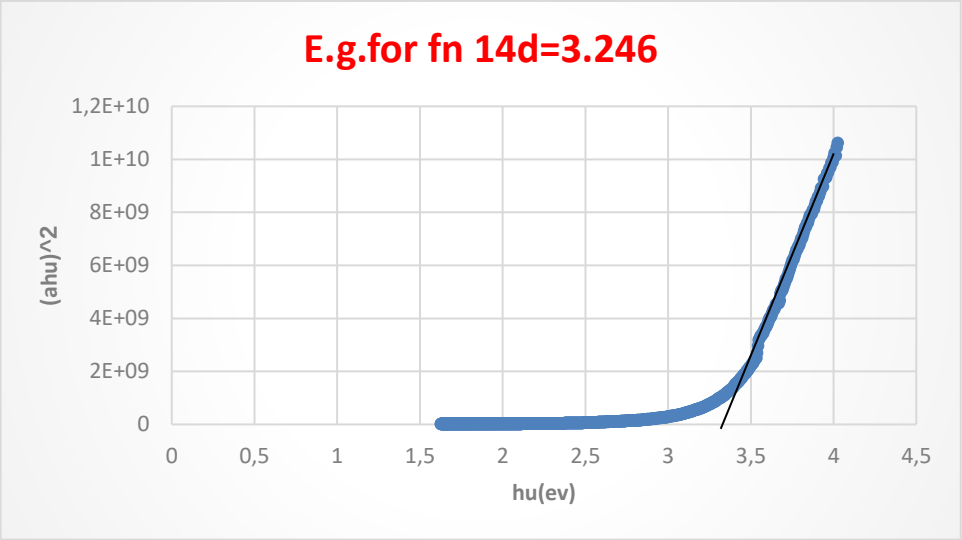

d)

Figure 0.1. a) Energy gap of pure, b) Energy gap of gamma, c) Energy gap of neutron, d) Energy gap of fast neutron.

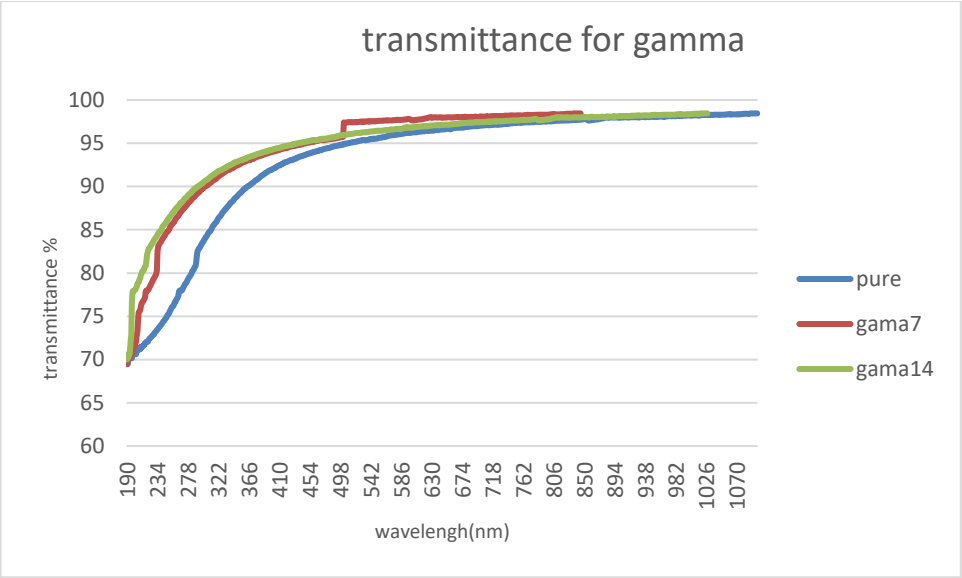

a)

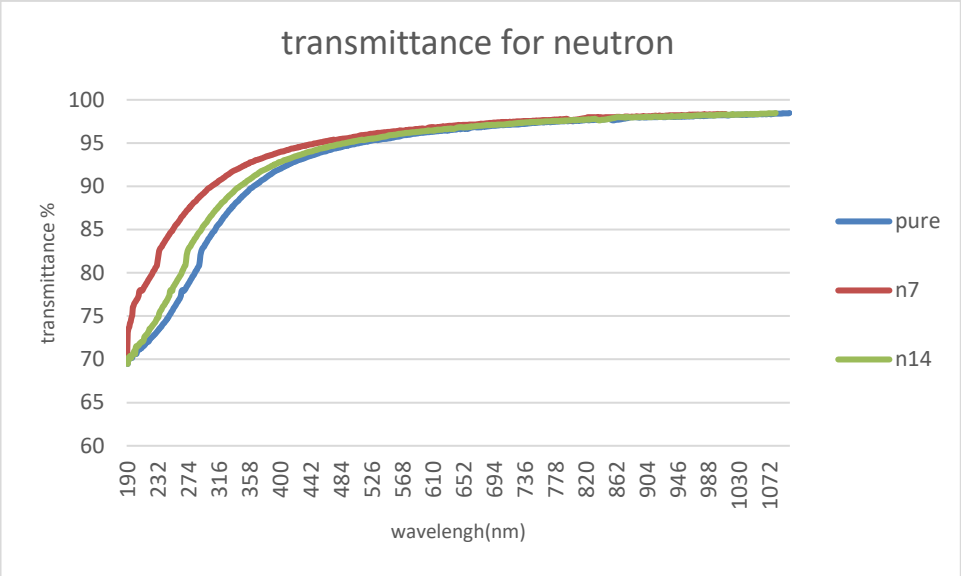

b)

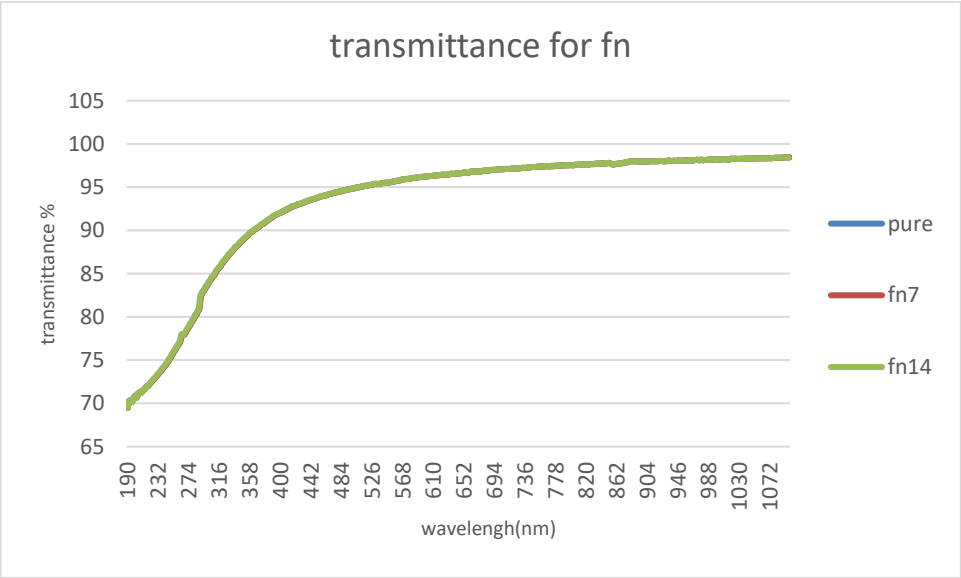

c)

Figure 0.2. a) Transmittance to gamma radiation, b)Transmittance to neutron radiation, c) Transmittance to fast neutron radiation.

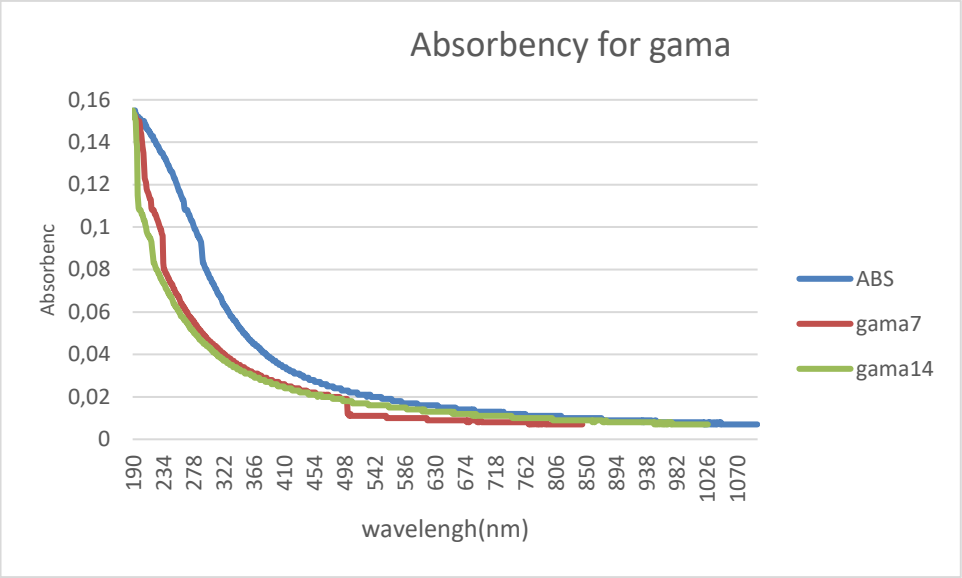
Absorbency for gama
0,16
0,14
0,12
0,1
0,08
0,06
0,04
0,02
0
Absorbenc
190
234
278
322
366
410
454
498
542
586
630
674
718
762
806
850
894
938
982
1026
1070
wavelengh(nm)
ABS
gama7
gama14

a)

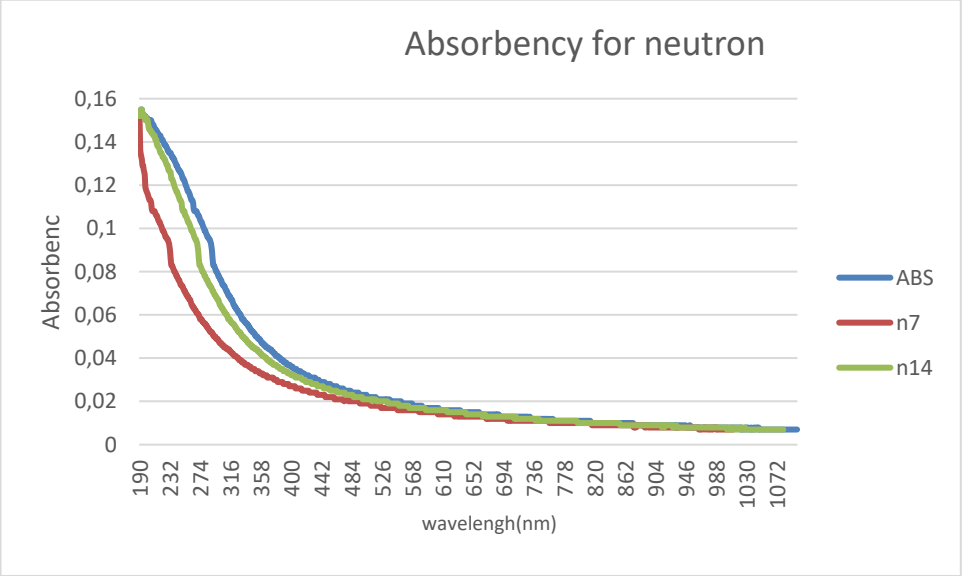
Absorbency for neutron
0,16
0,14
0,12
0,1
0,08
0,06
0,04
0,02
0
Absorbenc
190
232
274
316
358
400
442
484
526
568
610
652
694
736
778
820
862
904
946
988
1030
1072
wavelengh(nm)
ABS
n7
n14

b)

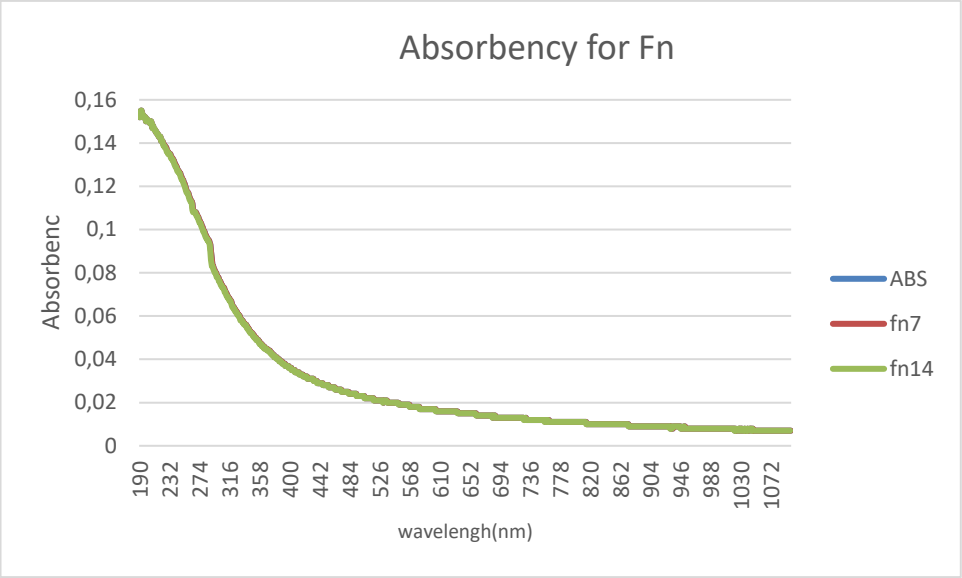

c)

Figure 0.3. a) Absorbance of gamma radiation, b) Absorbance of neutron radiation, c) Absorbance of fast neutron radiation.

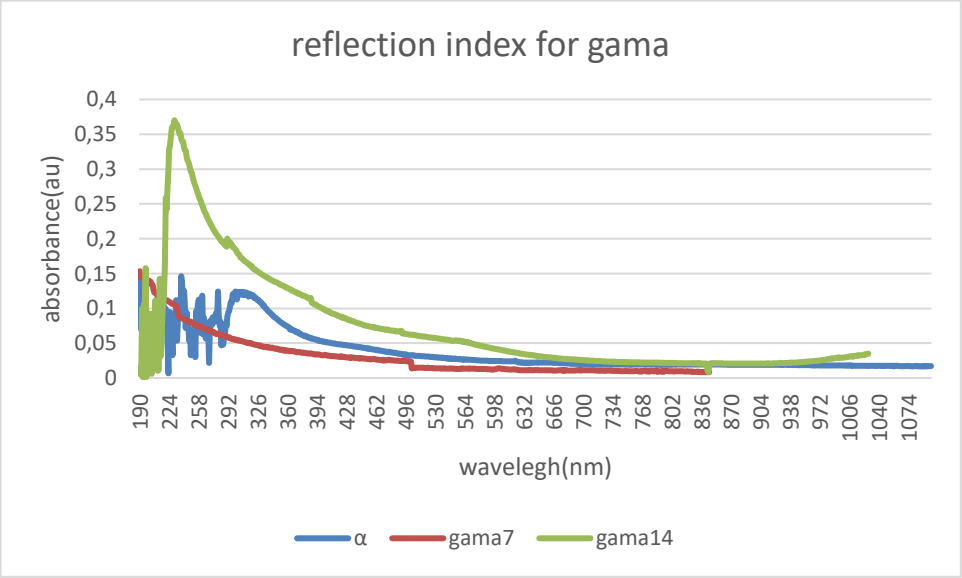

a)

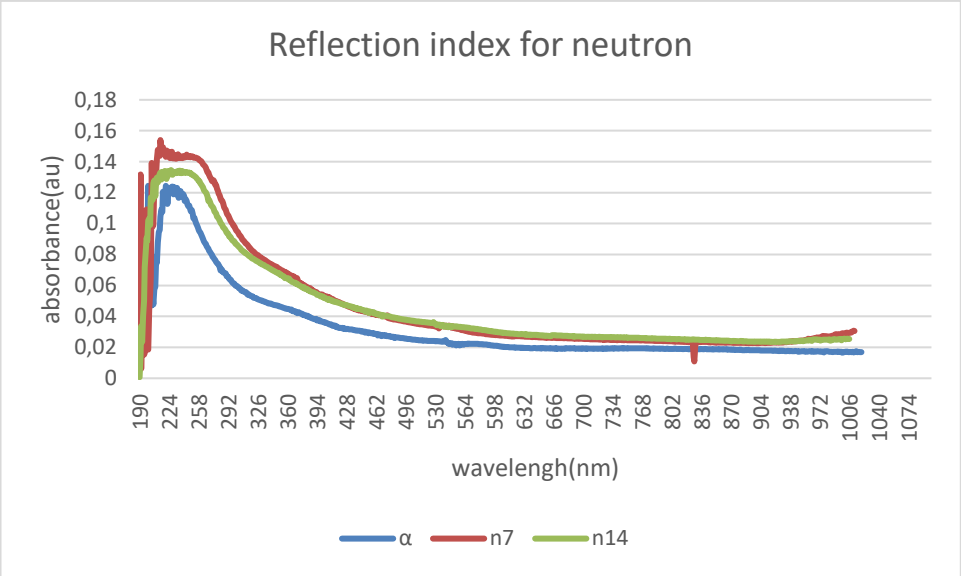

b)

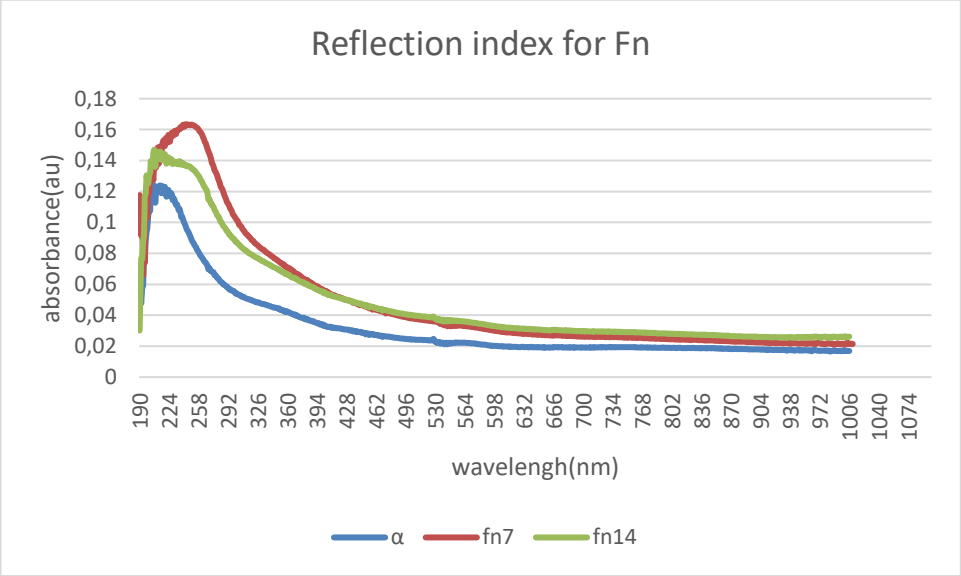

c)

Figure 0.4. a) Absorption coefficient for gamma rays, b) Absorption coefficient for neutron radiation, c) Absorption coefficient for fast neutron radiation.

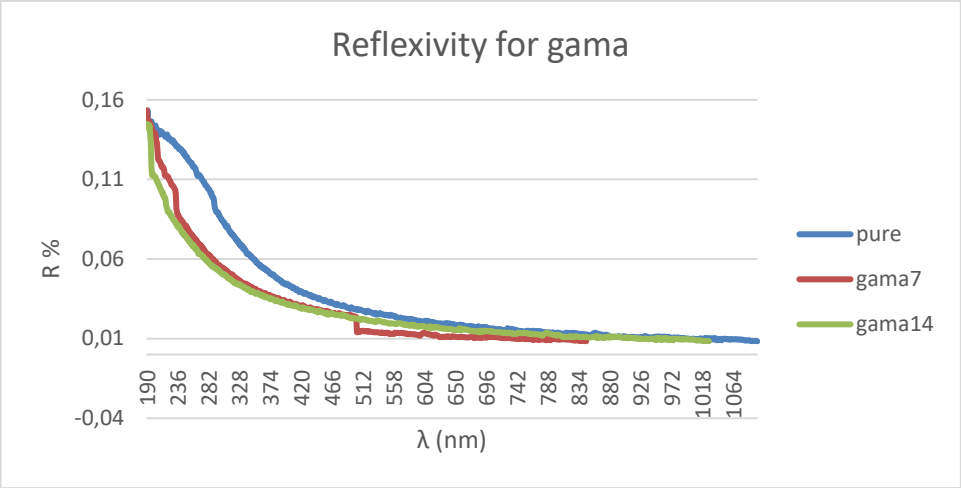

Figure 0.5. Reflectivity of gamma radiation.

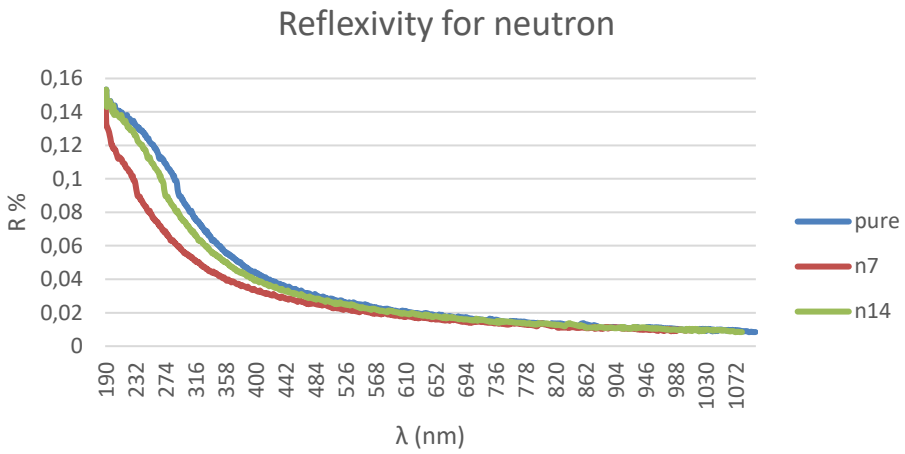

Figure 0.6. Reflectivity of neutron radiation.

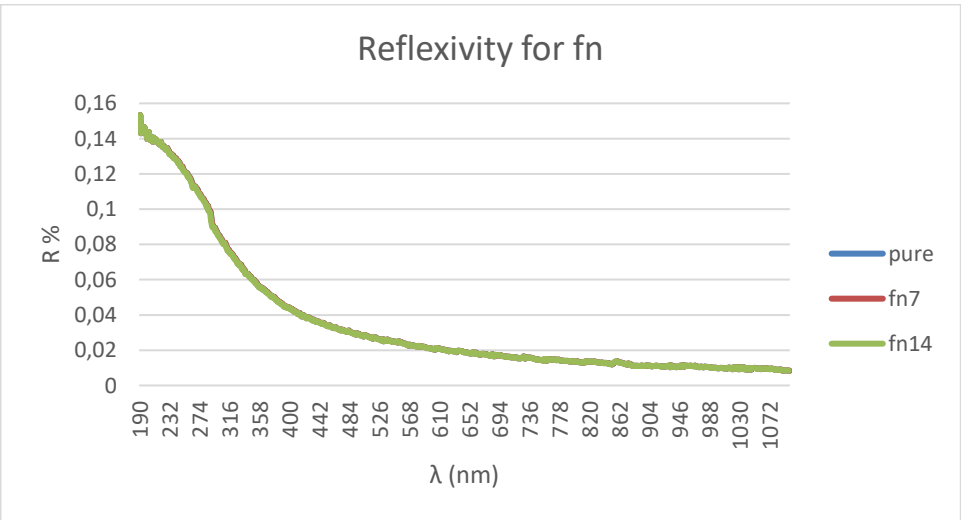

Figure 0.7. Reflectivity of fast neutron radiation.

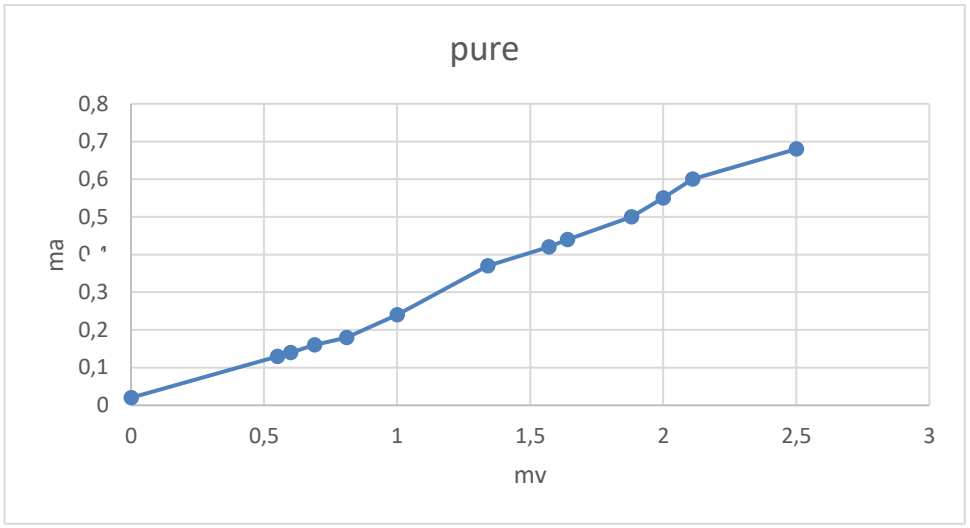
pure
0,8
0,7
0,6
0,5
0,3
0,2
0,1
0
ma
0
0,5
1
1,5
2
2,5
3
mv

a)

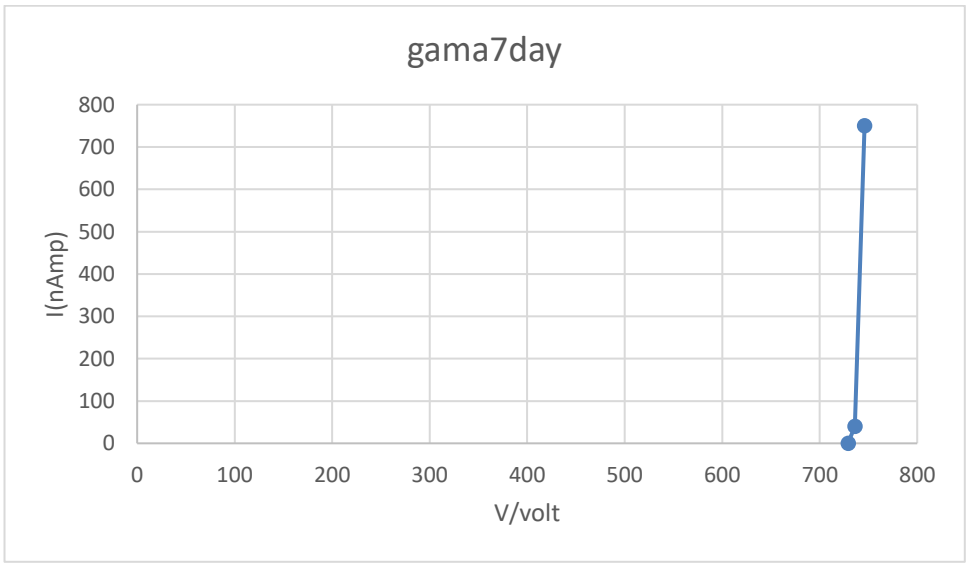
gama7day
800
700
600
500
400
300
200
100
0
I(nAmp)
0
100
200
300
400
500
600
700
800
V/volt

b)

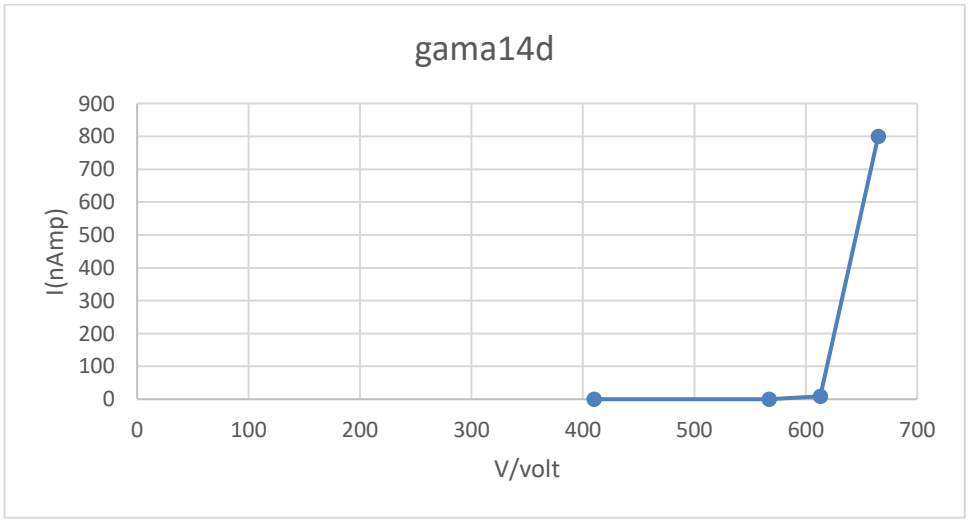
gama14d
900
800
700
600
500
400
300
200
100
0
I(nAmp)
0
100
200
300
400
500
600
700
V/volt

c)

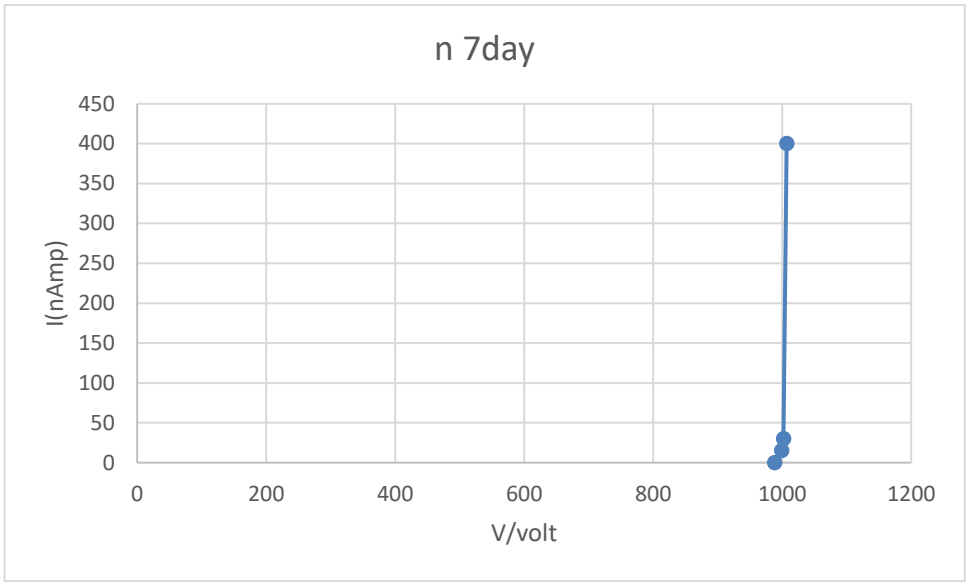
n 7day
450
400
350
300
250
200
150
100
50
0
I(nAmp)
0
200
400
600
800
1000
1200
V/volt

d)

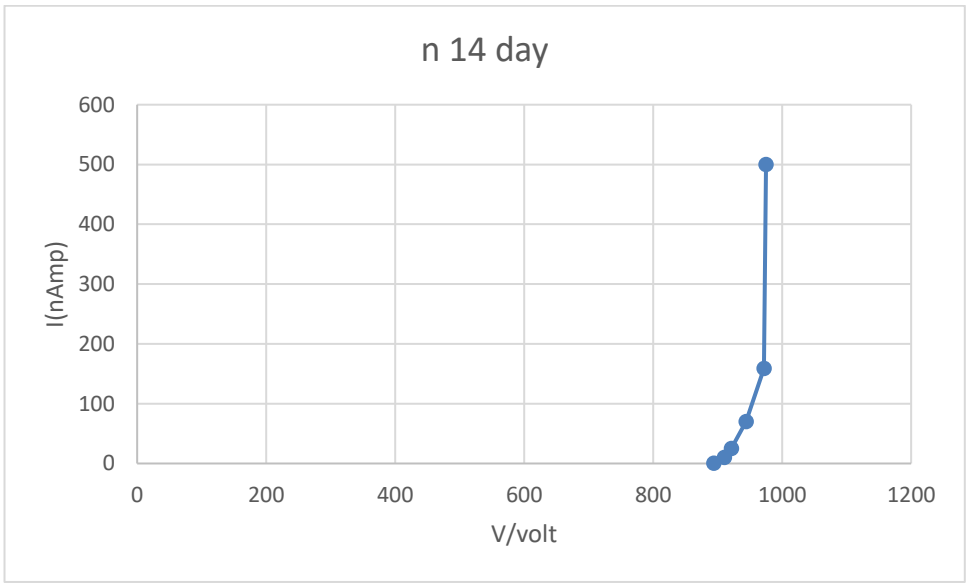
n 14 day
600
500
400
300
200
100
0
I(nAmp)
0
200
400
600
800
1000
1200
V/volt

e)

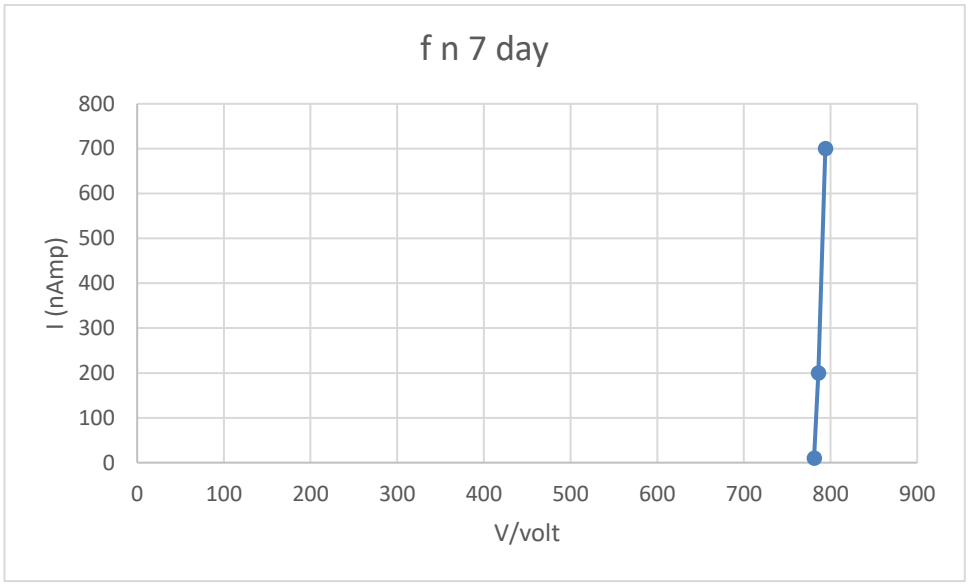

f)

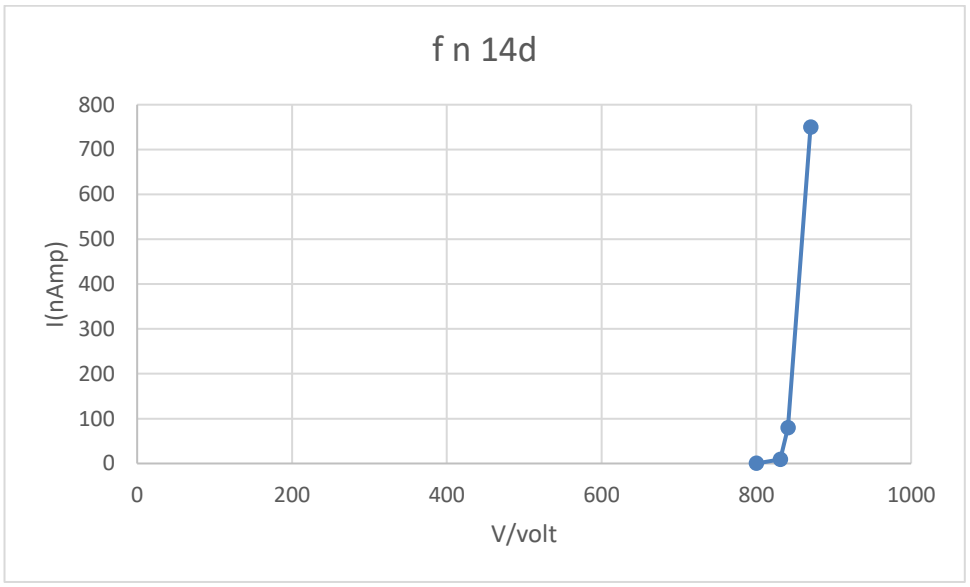

g)

Figure 0.8. a) Before irradiation, b) After irradiation with gamma rays for 7 days, c) After irradiation with gamma rays for 14 days, d) The thin film after.

irradiation with neutron radiation for 7 days, e) The thin film after irradiation with neutron radiation for 14 days, f) The thin film after irradiation with fast neutron radiation for 7 days, g) The thin film after irradiation with fast neutron radiation for 14 days.

Before irradiation, there was a crystalline structure, but after irradiation, the crystalline structure demolished.

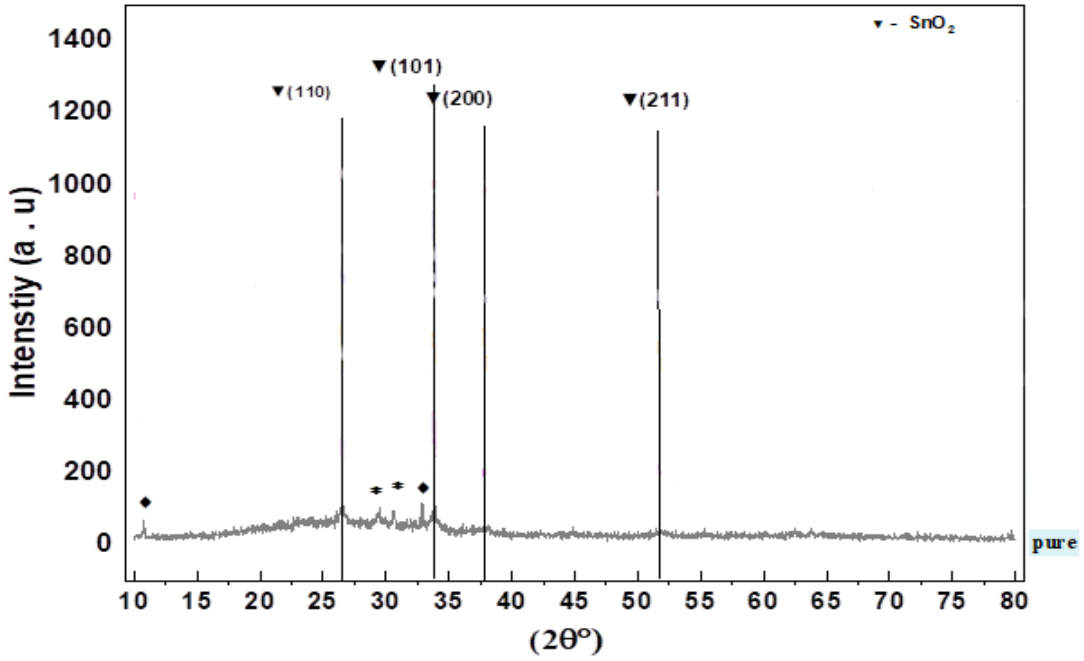
▼ - SnO2
▼(110)
▼(101)
▼(200)
▼(211)
Intenstiy (a . u)
1400
1200
1000
800
600
400
200
0
10 15 20 25 30 35 40 45 50 55 60 65 70 75 80
(2θ°)
pure

a)

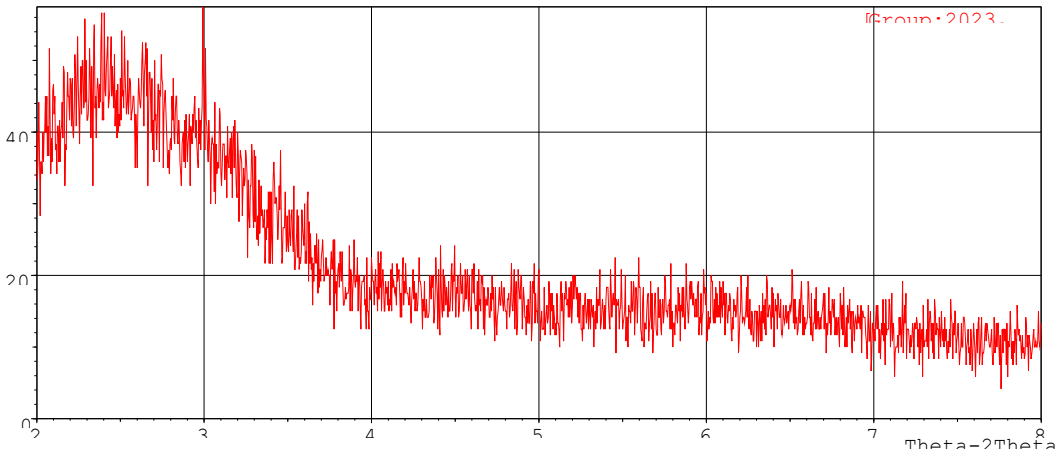
40
20
0
2 3 4 5 6 7 8
Theta-2Theta

b)

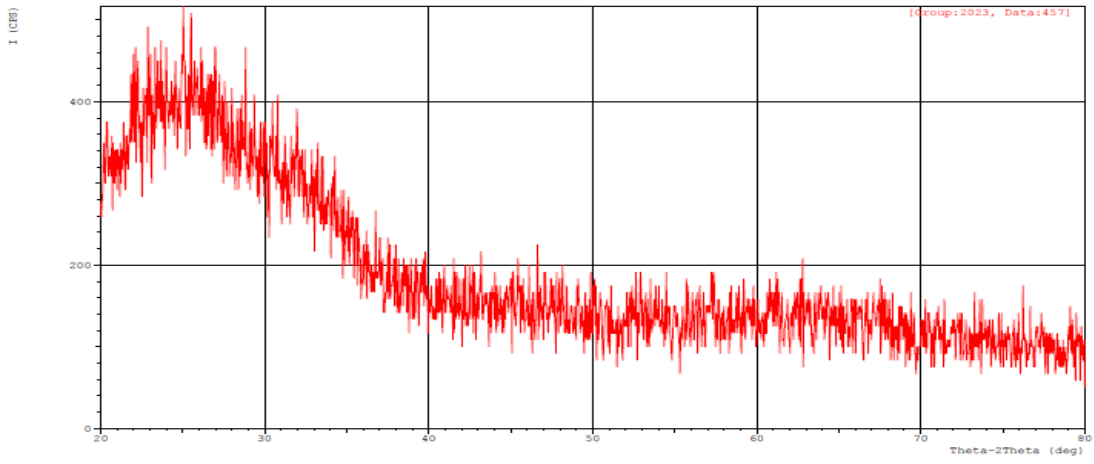
I (CPS)
400
200
0
20 30 40 50 60 70 80
Theta-2Theta (deg)

c)

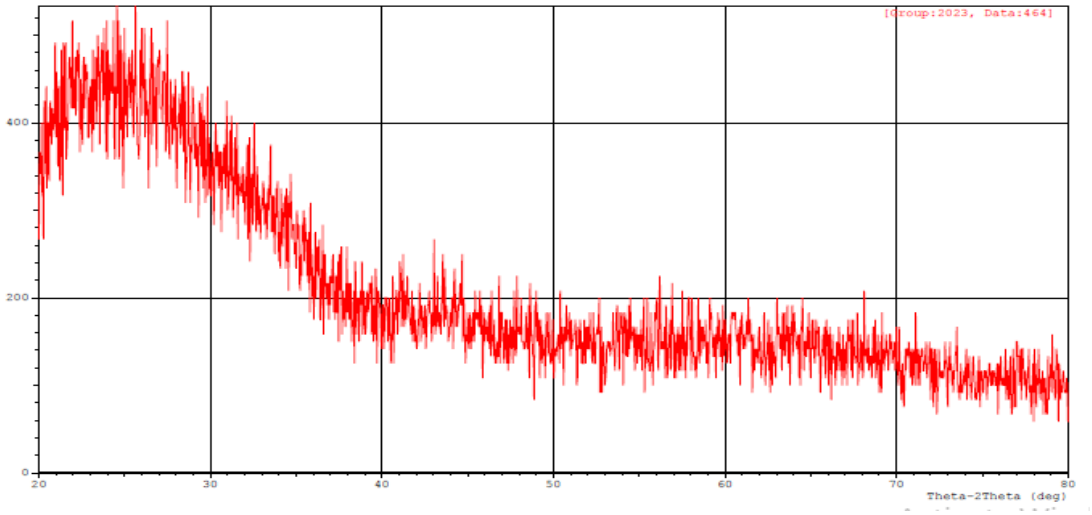
[Group:2023, Data:464]
400
200
0
20
30
40
50
60
70
80
Theta-2Theta (deg)

(d

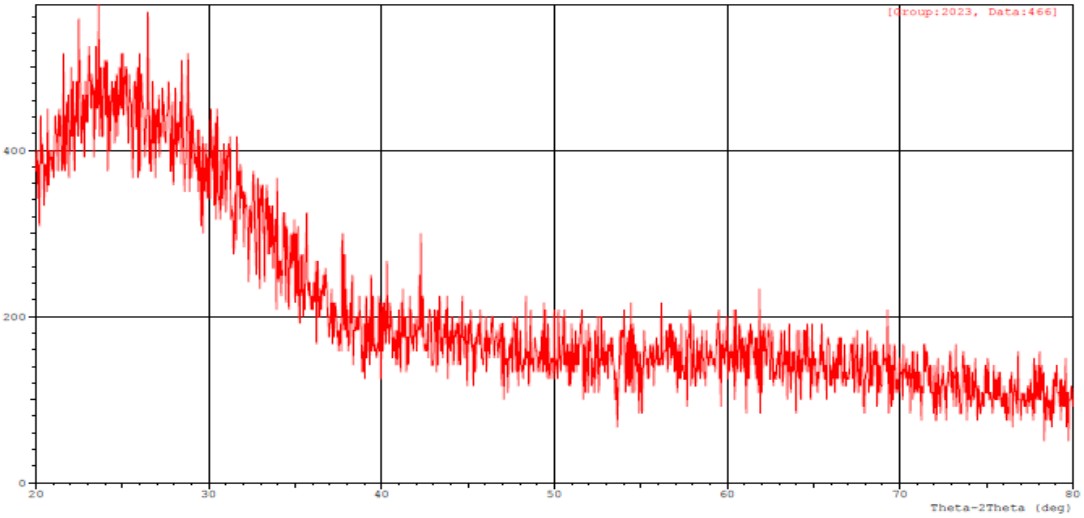
[Group:2023, Data:466]
400
200
0
20
30
40
50
60
70
80
Theta-2Theta (deg)

(e

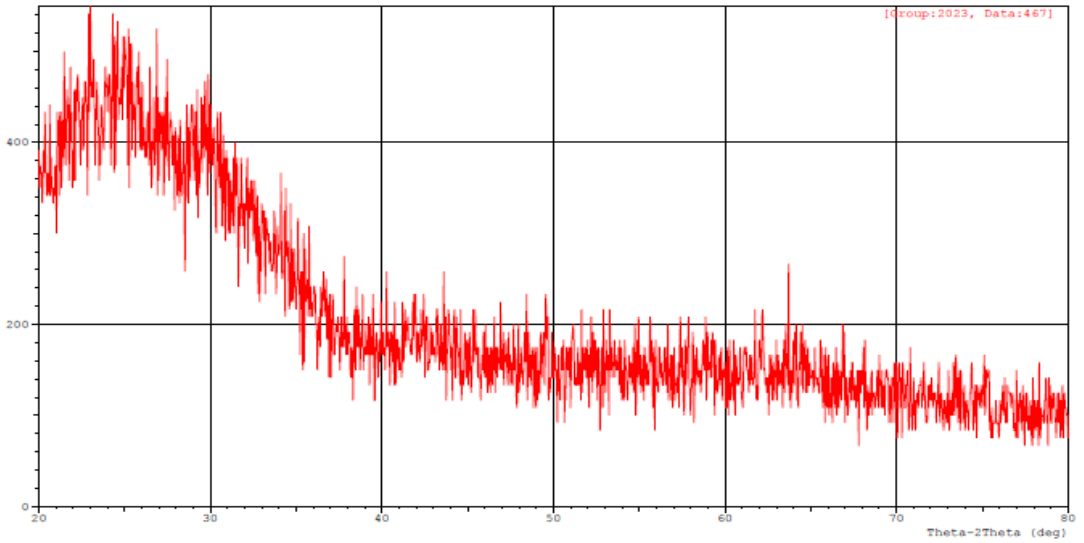
[Group:2023, Data:467]
400
200
0
20
30
40
50
60
70
80
Theta-2Theta (deg)

(f

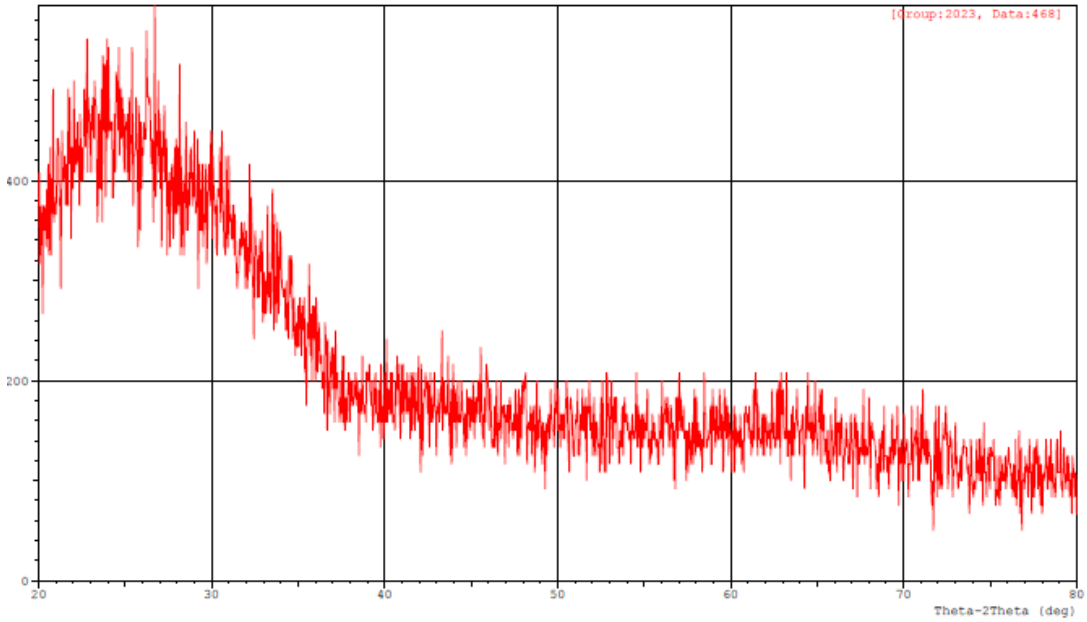

(g

Figure 5.9. A result of the electrical properties Before irradiation b), c), d), e), f), g) after irradiation with gamma and neutron

PART 6

CONCLUSIONS

Through this work, we can first observe the changes brought about by the irradiation process, especially the thermal neutrons, since the cross-section of the absorption of thermal neutrons by the tin material is 6.8 barns. Secondly, we can conclude that the irradiation process led to changing the prepared films from polycrystalline to amorphous at a low dose. 7 days, and with an increase in the radiation dose, it turns from polycrystalline to monocrystalline at 14 days, and this is what appeared and became an indicator of the change in optical properties such as transmittance, absorption, reflection, and absorption coefficients, and extinction coefficient. The energy gap was close and was less than the energy gap before irradiation. The reason is the possibility of changing the phase of the material after the irradiation process. As a conclusion, these changes can be invested in making or using this thin film in various fields as a sensor for thermal neutrons or as a radiation sensor a result of the response and appearance of the changes as confirmed by previous studies for other thin films [10] [11] [12].

In addition to the above, we conclude that this film affected irradiation, and this confirmed by XRD tests as a results of the film changing from polycrystalline to amorphous. Electrical tests also confirmed that the film affected by irradiation and its electrical properties changed so that the breakdown voltage in the range of 410 to 989 volts is the prevailing voltage for all thin films as a result of irradiation. Therefore, we conclude that this film affected the irradiation process, and we can benefit from the change in its optical, structural, or electrical properties to use it as a radiation sensor or in other applications.

REFERENCE

[1] S. M. Sze, “Semiconductors Devices Physics and Technology”, John Wiley_and Sons, Inc Publication, New York, (1990).

[2] J. S. Blakemore, *Solid State Physics*. Cambridge University Press, 1985.

[3] S. C. Tjong and H. Chen, “Nanocrystalline materials and coatings,” *Materials Science and Engineering: R: Reports*, vol. 45, no. 1, pp. 1–88, Sep. 2004, doi: 10.1016/j.mser.2004.07.001.

[4] S. M. Sze and K. K. Ng, *Physics of Semiconductor Devices*. John Wiley & Sons, 2006.

[5] S. C. Lofgran, “THIN FILM DEPOSITION & VACUUM TECHNOLOGY”.

[6] A. M. E.Ibrahim, R. A. Isma’el, E. S.Ibrahim, and E. M.Ibrahim, “Study the structural and Optical properties of ZnO thin film,” *Tikrit Journal of Pure Science*, vol. 22, no. 1, Art. no. 1, 2017, doi: 10.25130/tjps.v22i1.619.

[7] K.-D. Jäger, O. Isabella, A. H. M. Smets, R. A. C. M. M. van Swaaij, and M. Zeman, *Solar energy: fundamentals, technology and systems*. Cambridge: UIT Cambridge, 2016.

[8] Y.-L. Chang, “Epitaxial growth, characterization and solar cell application of indium nitride nanowires on silicon.” Accessed: Mar. 26, 2023. [Online]. Available: https://escholarship.mcgill.ca/concern/theses/c821gk740

[9] R. R. Hernandez *et al.*, “Environmental impacts of utility-scale solar energy,” *Renewable and Sustainable Energy Reviews*, vol. 29, pp. 766–779, Jan. 2014, doi: 10.1016/j.rser.2013.08.041.

[10] R. Lacal Arantegui and A. Jäger-Waldau, “Photovoltaics and wind status in the European Union after the Paris Agreement,” *Renewable and Sustainable Energy Reviews*, vol. 81, pp. 2460–2471, Jan. 2018, doi: 10.1016/j.rser.2017.06.052.

[11] H. Wang and Y. H. Hu, “Graphene as a counter electrode material for dye-sensitized solar cells,” *Energy Environ. Sci.*, vol. 5, no. 8, pp. 8182–8188, Jul. 2012, doi: 10.1039/C2EE21905K.

[12] A. Zribi and J. Fortin, *Functional Thin Films and Nanostructures for Sensors: Synthesis, Physics and Applications*. Springer Science & Business Media, 2009.

[13] “aldwayyan_c.v.pdf.” Accessed: Feb. 22, 2023. [Online]. Available: https://faculty.ksu.edu.sa/sites/default/files/aldwayyan_c.v.pdf

[14] “The Effect of Dielectric Nano Size on its some Electrical and Optical Properties.” Accessed: Feb. 24, 2023. [Online]. Available: https://repository.sustech.edu/handle/123456789/27635

[15] A. J. A. Fadlelmaula, -Mubarak Dirar Abdullah Supervisor, and -Ahmed Hassan Alfaki Co- Supervisor, “The Effect of Dielectric Nano Size on its some Electrical and Optical Properties,” Thesis, Sudan University of Science & Technology, 2022. Accessed: Feb. 24, 2023. [Online]. Available: https://repository.sustech.edu/handle/123456789/27635

[16] “Electron Beam Evaporation VS Thermal Evaporation,” Global Supplier of Sputtering Targets and Evaporation Materials | Stanford Advanced Materials. Accessed: Dec. 10, 2023. [Online]. Available: https://www.sputtertargets.net/blog/electron-beam-evaporation-vs-thermal-evaporation.html

[17] M. Ohring, *Materials Science of Thin Films: Depositon and Structure*. Elsevier, 2001.

[18] “Plane-strain Bulge Test for Thin Films | Journal of Materials Research | Cambridge Core.” Accessed: Feb. 25, 2023. [Online]. Available: https://www.cambridge.org/core/journals/journal-of-materials-research/article/abs/planestrain-bulge-test-for-thin-films/02847DE3BE6D3B35644F6FB5395F3105

[19] C. Jagadish and S. J. Pearton, *Zinc Oxide Bulk, Thin Films and Nanostructures: Processing, Properties, and Applications*. Elsevier, 2011.

[20] “Classification of thin film deposition methods | Surface Technology Journal | Ali Kosari Mehr,” KosarTech. Accessed: Dec. 23, 2023. [Online]. Available: https://kosartech.com/en/journal/posts/Classification-of-thin-film-deposition-methods

[1]Bahaa El-Din Hussein Marouf, Protection from ionizing radiation. Baghdad: Publications of the Iraqi Atomic Energy Organization, 1989

[22] “Alpha Beta And Gamma Radiation Mass,” All About Radiation. Accessed: Dec. 10, 2023. [Online]. Available: https://aboutradiation.blogspot.com/2020/03/alpha-beta-and-gamma-radiation-mass.html

[23] D. A. Mtlak and F. A. Aumran, “Study of background radiation in soil and water samples from many regions from Al-Fallujah city,” *IOP Conf. Ser.: Mater. Sci. Eng.*, vol. 928, no. 7, p. 072130, Nov. 2020, doi: 10.1088/1757-899X/928/7/072130.

[24] N. K. Abdalameer, “Effects of cold atmospheric plasma on the optical properties of SnO2 thin film,” 2017.

[25] S. J. Mohammed and Thair.KH.Salih, “A Study of structural and visual features of SnO2 membrane to be prepared Through Evaporation in Space,” *Tikrit*

Journal of Pure Science, vol. 18, no. 2, 2013, Accessed: Dec. 13, 2023. [Online]. Available: https://www.iasj.net/iasj/article/83833

[26] "Mus Alparslan University Journal of Science » Submission » Structural and morphological properties of SnO2:Sb:F thin films produced by spray pyrolysis technique at various substrate temperatures." Accessed: Dec. 21, 2023. [Online]. Available: https://dergipark.org.tr/en/pub/msufbd/issue/50934/648108

[69] "EBSCOhost | 144898076 | | 144898076 | Study of the optical properties of undoped and doped with antimony tin oxide films prepared using the techniqueAPCVD." Accessed: Dec. 21, 2023. [Online]. Available: https://web.s.ebscohost.com/abstract?direct=true&profile=ehost&scope=site&authtype=crawler&jrnl=1812125X&AN=144898076&h=BYsInZ73dvYbmNChGGBcKhc89FtX7Hj4DLtreySUtYAg%2bLL3HfDCfujtue%2fDayRjfUAsX0ELlk2ne%2fZMaophmw%3d%3d&crl=c&resultNs=AdminWebAuth&resultLocal=ErrCrlNotAuth&crlhashurl=login.aspx%3fdirect%3dtrue%26profile%3dehost%26scope%3dsite%26authtype%3dcrawler%26jrnl%3d1812125X%26AN%3d144898076

[28] A. Almuqrin, K. Mahmoud, and A. Abouhaswa, "Influence of increasing SnO2 content on the mechanical, optical, and gamma-ray shielding characteristics of a lithium zinc borate glass system," *Scientific Reports*, vol. 12, p. 1800, Feb. 2022, doi: 10.1038/s41598-022-05894-5.

[71] "Shamra Academy - a search engine for Arab academics | Deposition of tin oxide films using a continuous CO2 laser and their characterization.," Shamra Academia. Accessed: Dec. 21, 2023. [Online]. Available: http://shamra-academia.com/show/5998549009aa7

[30] K. N. Aklo, "Irradiation of the thin films of MnS with fast neutrons and the possibility of using the new characteristics in optical detector," *Energy Procedia*, vol. 157, pp. 290–295, Jan. 2019, doi: 10.1016/j.egypro.2018.11.193.

[31] N. F. Hububi, K. A. Mishjil, and M. H. Hassoni, "The Effict of y-Ray On The Optical Properties of (SnO2: Al) Thin Film," *Journal of College of Education*, no. 5, 2005, Accessed: Dec. 23, 2023. [Online]. Available: https://www.iasj.net/iasj/article/53195

[32] A. F. Maged, L. A. Nada, and M. Amin, "Effect of Gamma Radiation in Undoped SnO2 Thin Films," *Physical Science International Journal*, pp. 20–27, May 2015, doi: 10.9734/PSIJ/2015/17250.

[33] A. M. Al-Baradi *et al.*, "Tailoring the optical properties of tin oxide thin films via gamma irradiation," *Zeitschrift für Naturforschung A*, vol. 76, no. 12, pp. 1133–1146, Dec. 2021, doi: 10.1515/zna-2021-0215.

[34] R. Kajal, B. R. Kataria, K. Asokan, and D. Mohan, "Effects of gamma radiation on structural, optical, and electrical properties of SnO2 thin films," *Applied Surface Science Advances*, vol. 15, p. 100406, Jun. 2023, doi: 10.1016/j.apsadv.2023.100406.

[35] P. A. Thiel and T. E. Madey, “The interaction of water with solid surfaces: Fundamental aspects,” *Surface Science Reports*, vol. 7, no. 6, pp. 211–385, Oct. 1987, doi: 10.1016/0167-5729(87)90001-X.

[36] S. M. Sze and K. K. Ng, *Physics of Semiconductor Devices*. John Wiley & Sons, 2006.

[29] S. Sze ،“semiconductors devices physics and technology” ،translated by Dr. F. Hayaty and Dr. H. A ،Ahmed ،Al-Mosual University ،press ،(1990).

[30] Kittel ،C. ،& McEuen ،P. (2018). Introduction to solid state physics. John Wiley & Sons.

[39] B. G. Streetman and S. Banerjee, *Solid state electronic devices*, vol. 4. Prentice hall New Jersey, 2000. Accessed: Dec. 18, 2023. [Online]. Available: https://www.researchgate.net/profile/Ajay_Kumar531/post/Can_the_Fermi_energy_cross_the_conduction_band_in_n-type_semiconductor/attachment/609536106b9531000149f157/AS%3A1020809837555714%401620391439350/download/Solid_State_Electronic_Devices_by_Ben_Streetman+7th+edition.pdf

[40] B. G. Streetman and S. Banerjee, *Solid state electronic devices*, 5th ed. in Prentice-Hall series in solid state physical electronics. Upper Saddle River, N.J.: Prentice Hall, 2000.

[41] “X-Ray Diffraction Procedures: For Polycrystalline and Amorphous Materials, 2nd Edition | Wiley,” Wiley.com. Accessed: Mar. 03, 2023. [Online]. Available: https://www.wiley.com/en-us/X+Ray+Diffraction+Procedures%3A+For+Polycrystalline+and+Amorphous+Materials%2C+2nd+Edition-p-9780471493693

[42] *Thin Film Techniques and Applications*. Allied Publishers, 2004.

[43] “Is MgO an intrinsic N-type or P-type semiconductor?,” ResearchGate. Accessed: Dec. 24, 2023. [Online]. Available: https://www.researchgate.net/post/Is_MgO_an_intrinsic_N-type_or_P-type_semiconductor

[44] J. S. Blakemore, *Solid State Physics*. Cambridge University Press, 1985.

[45] B. E. Warren, *X-ray Diffraction*. Courier Corporation, 1990.

[46] S. M. Sze and K. K. Ng, *Physics of Semiconductor Devices*. John Wiley & Sons, 2006.

[47] M. Anitha, K. Saravanakumar, N. Anitha, and L. Amalraj, “Influence of fluorine doped CdO thin films by an simplified spray pyrolysis technique using nebulizer,” *Opt Quant Electron*, vol. 51, no. 6, p. 187, May 2019, doi: 10.1007/s11082-019-1901-1.

[48] G. Aksoy, “The Effects of Animation Technique on the 7th Grade Science and Technology Course,” *CE*, vol. 03, no. 03, pp. 304–308, 2012, doi: 10.4236/ce.2012.33048.

[39] M. a. Suleiman, A. F. Pasha, and Sh. a. Khairy, Solid State Physics, ed. 1. In the Arabic Thought Series for Basic Science References. Cairo: Dar Al-Fikr Al-Arabi, 2000.

[50] D. B. Holt and B. G. Yacobi, *Extended Defects in Semiconductors: Electronic Properties, Device Effects and Structures*. Cambridge University Press, 2007.

[51] “Figure 2.8: Schematic drawing of (a) the typical Scanning Electron...,” ResearchGate. Accessed: Dec. 26, 2023. [Online]. Available: https://www.researchgate.net/figure/Schematic-drawing-of-a-the-typical-Scanning-Electron-Microscope-SEM-column-170_fig5_281184428

[52] A. Abd, “Quantum dots CdSe/PSi/Si Photodetector,” 2015. doi: 10.13140/RG.2.2.12332.26241.

[53] E. V. Dubrovin, O. N. Koroleva, Y. A. Khodak, N. V. Kuzmina, I. V. Yaminsky, and V. L. Drutsa, “AFM study of Escherichia coli RNA polymerase σ70 subunit aggregation,” *Nanomedicine: Nanotechnology, Biology and Medicine*, vol. 8, no. 1, pp. 54–62, Jan. 2012, doi: 10.1016/j.nano.2011.05.014.

[54] L. Feng, A. Liu, Y. Ma, M. Liu, and B. Man, “Fabrication, Structural Characterization and Optical Properties of the Flower-Like ZnO Nanowires,” *Acta Phys. Pol. A*, vol. 117, no. 3, pp. 512–517, Mar. 2010, doi: 10.12693/APhysPolA.117.512.

[55] L. Feng, A. Liu, M. Liu, Y. Ma, J. Wei, and B. Man, “Synthesis, characterization and optical properties of flower-like ZnO nanorods by non-catalytic thermal evaporation,” *Journal of Alloys and Compounds*, vol. 492, no. 1, pp. 427–432, Mar. 2010, doi: 10.1016/j.jallcom.2009.11.129.

[45] S. S. Al-Rawi ،S. J. Shakir and Y. N. Husan ،“Solid State Physics” Book،Al-Mousal University Press ،Arabic Version ،(1990).

[57] J.-P. Colinge and C. A. Colinge, *Physics of Semiconductor Devices*. Springer Science & Business Media, 2005.

[58] P. A. Thiel and T. E. Madey, “The interaction of water with solid surfaces: Fundamental aspects,” *Surface Science Reports*, vol. 7, no. 6, pp. 211–385, Oct. 1987, doi: 10.1016/0167-5729(87)90001-X.

[59] “Tracing the 5000-year recorded history of inorganic thin films from ∼3000 BC to the early 1900s AD: Applied Physics Reviews: Vol 1, No 4.” Accessed: Mar. 11, 2023. [Online]. Available: https://aip.scitation.org/doi/abs/10.1063/1.4902760

[60] O. Stenzel, *The physics of thin film optical spectra: an introduction*. in Springer series in surface sciences, no. 44. Berlin ; New York: Springer, 2005.

[61] M. K. Erhaima, “Structural and Optical Properties of ZnO:Co)CZO(Thin Films Prepared by Chemical Spray Pyrolysis Method”.

[62] D. A. Neamen, *Semiconductor physics and devices : basic principles*. McGraw-Hill, 2003. Accessed: Mar. 14, 2023. [Online]. Available: http://repository.vnu.edu.vn/handle/VNU_123/91335

[63] J. I. Pankove, *Optical Processes in Semiconductors*. Courier Corporation, 1975.

[64] “Polycrystalline And Amorphous Thin Films And Devices - كتب Google.” Accessed: Mar. 15, 2023. [Online]. Available: https://books.google.iq/books?hl=ar&lr=&id=40tj3r8rEmcC&oi=fnd&pg=PA135&dq=Clark%D8%8C+A.+H.+(1980).+Optical+properties+of+polycrystalline+semiconductor+films.+Polycrystalline+and+Amorphous+Thin+Films+and+Devices%D8%8C+135-152.%E2%80%8F&ots=FaMjTDXzNP&sig=Z2-JFEC9Gml3u2KWcJ_n61Xg80M&redir_esc=y#v=onepage&q&f=false

[65] “Polycrystalline And Amorphous Thin Films And Devices - كتب Google.” Accessed: Mar. 16, 2023. [Online]. Available: https://books.google.iq/books?hl=ar&lr=&id=40tj3r8rEmcC&oi=fnd&pg=PA135&dq=Clark%D8%8C+A.+H.+(1980).+Optical+properties+of+polycrystalline+semiconductor+films.+Polycrystalline+and+Amorphous+Thin+Films+and+Devices%D8%8C+135-152&ots=FaMkKB-CMP&sig=6EX1q3m4by23HlbVJTqc322s78U&redir_esc=y#v=onepage&q&f=false

[66] B. Klug, “Intel’s 50Gbps Silicon Photonics Link: The Future of Interfaces.” Accessed: Dec. 27, 2023. [Online]. Available: https://www.anandtech.com/show/3834/intels-silicon-photonics-50g-silicon-photonics-link

[67] “Solid State Physics - Giuseppe Grosso, Giuseppe Pastori Parravicini - كتب Google.” Accessed: Mar. 16, 2023. [Online]. Available: https://books.google.iq/books?hl=ar&lr=&id=ZJzmUAp0hMcC&oi=fnd&pg=PR1&dq=Grosso%D8%8C+G.%D8%8C+%26+Parravicini%D8%8C+G.+P.+(2013).+Solid+state+physics.+Academic+press&ots=H1UMojLaqS&sig=H_n03pCkfEaFcG0z3swhmwZDSyE&redir_esc=y#v=onepage&q=Grosso%D8%8C%20G.%D8%8C%20%26%20Parravicini%D8%8C%20G.%20P.%20(2013).%20Solid%20state%20physics.%20Academic%20press&f=false

[68] C. F. Niedik, C. Freye, F. Jenau, D. Haring, G. Schroder, and J. Bittmann, “Investigation on the electrical characterization of silicone rubber using DC conductivity measurement,” *2016 IEEE International Conference on Dielectrics (ICD)*, pp. 1114–1118, Jul. 2016, doi: 10.1109/ICD.2016.7547814.

[69] C. F. Niedik, C. Freye, F. Jenau, D. Häring, G. Schröder, and J. Bittmann, “Investigation on the electrical characterization of silicone rubber using DC conductivity measurement,” in *2016 IEEE International Conference on Dielectrics (ICD)*, Jul. 2016, pp. 1114–1118. doi: 10.1109/ICD.2016.7547814.

[70] C. Kittel and P. McEuen, *Introduction to Solid State Physics*. John Wiley & Sons, 2018.

[71] "2.7 Carrier transport." Accessed: Dec. 27, 2023. [Online]. Available: https://truenano.com/PSD20/chapter2/ch2_7.htm

[72] "Is the resistance of a diode without voltage applied the same when measured in reverse and forward?," Quora. Accessed: Dec. 26, 2023. [Online]. Available: https://www.quora.com/Is-the-resistance-of-a-diode-without-voltage-applied-the-same-when-measured-in-reverse-and-forward

[73] S. J. Ikhmayies and R. N. Ahmad-Bita, "Effect of Processing on the Electrical Properties of Spray-Deposited SnO2:F Thin Films," *American J. of Applied Sciences*, vol. 5, no. 6, pp. 672–677, Jun. 2008, doi: 10.3844/ajassp.2008.672.677.

[74] J. Joseph, V. Mathew, J. Mathew, and K. E. Abraham, "Studies on Physical Properties and Carrier Conversion of SnO_2:Nd Thin Films," *Turkish Journal of Physics*, Jan. 2009, doi: 10.3906/fiz-0707-4.

[75] H. Huang, O. K. Tan, Y. C. Lee, and M. S. Tse, "Preparation and characterization of nanocrystalline SnO2 thin films by PECVD," *Journal of Crystal Growth*, vol. 288, no. 1, pp. 70–74, Feb. 2006, doi: 10.1016/j.jcrysgro.2005.12.031.

[76] Y. Lu, "SnO2 thin films - chemical vapor deposition and characterization".

[77] "Structural and Optical Properties of SnO2 Films Grown on 6H-SiC by MOCVD | Scientific.Net." Accessed: Feb. 27, 2023. [Online]. Available: https://www.scientific.net/AMR.79-82.1539

[78] "Thermal Evaporation - an overview | ScienceDirect Topics." Accessed: Dec. 12, 2023. [Online]. Available: https://www.sciencedirect.com/topics/chemistry/thermal-evaporation

[79] Study of Structural and Optical Properties of (ZnO:Sn)Thin Films Prepared By Chemical Spray Pyrolysis Method." Accessed: Dec. 23, 2023. [Online]. Available: https://iqdr.iq/search?view=257c0c51791f7bc8a221fa9ddb0c8f43

RESUME

Abdulrahman Faaiq Dawood AL-BADRY he graduated from Al khatib Boys' Hight School in 2017. Graduated from Tikrit University/ Faculty of Science/ department of Physics, which started in 2017. Graduated in 2021 and started graduate studies at Karabuk University in the state of science department of physics.